University Research Initiative

Fate and Effects of N-, O-, and S- Heterocycles (NOSHs) from Petroleum and Pyrogenic Sources in Marine Sediments

MMS **U.S. Department of the Interior**
Minerals Management Service
Gulf of Mexico OCS Region

(LUMCON)

Cooperative Agreement
University Research Initiative
Louisiana Universities Marine Consortium

University Research Initiative

Fate and Effects of N-, O-, and S- Heterocycles (NOSHs) from Petroleum and Pyrogenic Sources in Marine Sediments

Authors

W. James Catallo
Laboratory for Ecological Chemistry and Toxicology
VPT, School of Veterinary Medicine
Louisiana State University
Baton Rouge, Louisiana

and

Robert P. Gambrell
Wetland Biogeochemistry Institute
Louisiana State University
Baton Rouge, Louisiana

February 1995

DISCLAIMER

This report was prepared under contract between the Minerals Management Service (MMS) and the Louisiana Universities Marine Consortium (LUMCON). This report has been technically reviewed by the MMS and approved for publication. Approval does not signify that the contents necessarily reflect the views and policies of the Service, nor does the mention of trade names or commercial products constitute endorsement or recommendation for use. It is, however, exempt from review and compliance with MMS editorial standards.

REPORT AVAILABILITY

Extra copies of this report may be obtained from the Public Information Unit (Mail Stop 5034) at the following address:

CITATION

Suggested citation:

Catallo, W. James and R. P. Gambrell. 1995. Fates and Effects of N-, O-, and S- Heterocycles (NOSHs) from Petroleum and Pyrogenic Sources in Marine Sediments. OCS Study MMS 94-0056. U.S. Dept. of the Interior, Minerals Mgmt. Service, Gulf of Mexico OCS Region, New Orleans, La. 72 pp.

ABSTRACT

The purpose of this work was to examine the chemistry of N-, O-, and S- heterocycles (NOSHs) from fossil fuels and pyrogenic sources in estuarine sediment-water with emphasis on relative rates and pathways of transformation. The effects of redox potential (Eh) and sediment particle size on NOSH degradation were examined using a) stirred, controlled Eh sediment-water microcosms and, b) sealed, unstirred batch vial microcosms approximating natural sediments. These experiments were accompanied by characterization of NOSH transformation products using mass spectrometry, molecular modelling of NOSH reactions and chromatographic behavior, and toxicological evaluation of NOSHs and their transformation products. Complex suites of NOSH transformation products were identified in extracts from both types of microcosm. Selected NOSH compounds showing transformation to stable products were synthesized in deuterated form, and tracer experiments were conducted to confirm the data from product analysis and postulate mechanisms of degradation and/or toxicity. Microbes degrading the NOSHs were isolated, characterized, and then used in degradation pathway determination. Results from the controlled Eh microcosms showed that most of the 19 NOSHs examined were transformed in the mixed sediment slurries under both oxidized and reduced conditions, and the transformation product distributions were very similar in all treatments. An important factor in the degradation of the NOSHs was sediment particle size: rates and extent of degradation generally decreased with decreasing particle size (i.e., increasing total surface area). Reduced redox conditions also were associated with slower rates of NOSH transformation vs. oxidized sediments, but this effect was somewhat attenuated by the physicochemical effects of constant stirring. The cytotoxicity of aqueous phase samples from the oxidized microcosms generally decreased with time and progressive NOSH degradation. The level of measured aqueous cytotoxicity, however, oscillated before becoming consistently low. The nonlinearity of aqueous toxicity profiles over time suggested that toxic transformation products were generated during the degradation of the NOSHs in the aqueous phase. This also was observed to a lesser extent in the aqueous phases of the reduced microcosms, but background toxicity was high in these systems and changes over time were less pronounced than oxidized water samples. Comparative NOSH degradation experiments also were run in unstirred microcosms under oxidized and reduced conditions. These systems allowed no tight control of Eh conditions, and were intended to more closely emulate field conditions than the controlled Eh/pH microcosms. Many of the NOSHs examined in these unstirred systems did not degrade substantially. Like the stirred microcosms, NOSH degradation proceeded more slowly and on fewer compounds in fine grained clay than in coarser grained sand and silt. Unlike the stirred systems, however, reduced redox conditions clearly favored NOSH compound degradation relative to oxidized conditions. Empirical and theoretic data suggested that this redox effect was related to the tendency of many NOSHs to form stable metal complexes with iron and perhaps other metals in situ. Under reducing conditions, desorption of redox active metals (e.g., Fe) from sediment sites would liberate complexed NOSHs to the aqueous phase, where relatively rapid chemical and biological degradtaion processes occurred. Results of pathway studies and deuterated tracer experiments on the NOSHs showed that a complex suite of transformation reactions occurred in the microcosms. These included a) chemical and biological oxidation of aromatic rings to phenols, ketones, and epoxides, b) disproportionation, saturation and opening of benzylic rings, c) oxidation of alkyl side chains followed by decarboxylation, d) oxidation of heterocyclic sulfur to sulfoxides and sulfones, e) addition reactions (alkylation, glycoaldehyde addition) and, f) β oxidation of broken rings and side chains.

TABLE OF CONTENTS

LIST OF FIGURES

LIST OF TABLES

LIST OF ACRONYMS AND ABBREVIATIONS

The following acronyms are used in this report:

AZAFLUOR	4-azafluroene
BENZQUIN	Benzo(f)quinoline
BP	Boiling point
BTHIAZOL	Benzothiazole
BTHIOPH	2,3-benzothiophene
CV	Coefficient of variation
D	Dipole moment
DBFURAN	Dibenzofuran
DBPYRAN	Dibenzopyran
DCM	Dichloromethane
DMSO	Dimethylsulfoxide
DMQUINOX	2,3-dimethylquinoxaline
DMS	Dimethylsulfide
DNA	Deoxyribosenucleic acid
FID	Flame ionization detector
Hf	Heat of formation
GC	Gas chromatograph
GC-MS	Gas chromatograph mass spectrometer
Log P	Log octanol:water partition coefficient
m/z	Mass to charge ratio
MECARBAZ	9-methylcarbazole
MVOL	Molar volume
MQUIN_2	2-methylquinoline
MQUIN_3	3-methylquinoline
MQUIN_4	4-methylquinoline
MQUIN_8	8-methylquinoline
MSAR	Molecular surface area
MW	Molecular weight
NOSHs	N-, O-, S-, heterocycles
OX	Oxidized
PHENANTH	Phenanthridine
POLAR	Total molecular polar surface area
QUIN_C2	2,4-dimethylquinoline
QUIN_CN	3-quinolinecarbonitrile
QUINOLIN	Quinoline
QUINOXAL	Quinoxaline
QQ	Total molecular charge-charge repulsion energy
RED	Reduced
RT (Rt)	Retention time
SATUR	Total saturated molecular surface area
SURR	Surrogate Standard
TOTSA	Total molecular surface area
Tor	Total molecular torsion energy
UNSAT	Total unsaturated molecular surface area
VDW	Van der Waals energy

ACKNOWLEDGEMENTS

INTRODUCTION

N-, O-, and S- heterocycles (NOSHs) are polycyclic aromatic compounds containing one or more N-, O-, and/or S- atoms in five or six membered rings (Figure 1). These include condensed ring systems based on indole, pyridine, thiophene, furan, and pyran. NOSHs are found in polar and asphaltic fractions of crude petroleum, produced waters, oil field tars and sludges, shale oils, coal synfuels, and pyrogenic products (Catallo et al. 1990a, Thompkins and Ho 1982; Krone et. al. 1986, Wakeham 1979; Furlong and Carpenter 1982; Beiko et al. 1987; Stetter et al. 1985; Yamaguchi and Handa 1987; Turov et al. 1987; Wolfe 1977). In the few studies specifically addressing them, NOSHs of low and intermediate molecular weight generally were found to be more mobile in sediment-water systems than analogous polycyclic aromatic hydrocarbons (PAHs), and more resistant to degradation by chemical, photochemical, and microbial processes (Jorgensen et al. 1985; Sumskaya and Varfolomeyev 1988; Smith et al. 1977, 1978; Stetter et al. 1985). An interesting property of some NOSHs is that they can complex or otherwise interact with soluble metals such as Fe^{2+}, Mn^{2+}, and Ca^{2+} or protonate at sediment surfaces and enter the aqueous phase (Catallo et al. 1994; Jorgensen et al. 1985; Stetter et al. 1985; Haugen et al. 1982). This has been shown to increase the leachability of NOSHs through compositionally heterogeneous sediment profiles, and has been implicated as a mechanism of their cytotoxicity (Catallo et al., 1990a, 1992a, 1994). The results of one study suggested that quinoline, and probably other pyridine-based azaarenes are not oxidized during complexation with Mn^{2+} and Fe^{2+}, as has been observed for aromatic amines and certain refractile chlorinated compounds (Laha and Luthy, 1990).

Currently there are no data available on NOSH degradation processes in marine sediments of different composition and/or physicochemical properties. A few studies have documented the degradation of small numbers of NOSHs in estuarine water and sewage sludges (Chou and Bohonos 1979; Black et al. 1993), but data sediment fates are not readily available. The effects of sediment electrochemical conditions (redox potential or "Eh"), particle size distribution, and organic matter content on chemical and biological transformation of NOSHs are unknown (Ponnamperumma 1972). Nevertheless, the presence of extended series of NOSH compounds in riverine and marine sediments suggests that their degradation *in situ* is slow (Blumer 1975; Lopez-Avila and Hites 1980; Zitko 1980). Other work has shown the presence of extended NOSH series including thiophenes, thiazoles, furans, and pyrans in sediments and benthic biota from Lake Pontchartrain (McFall et al. 1985).

The toxicology of NOSHs also is insufficiently documented.

1
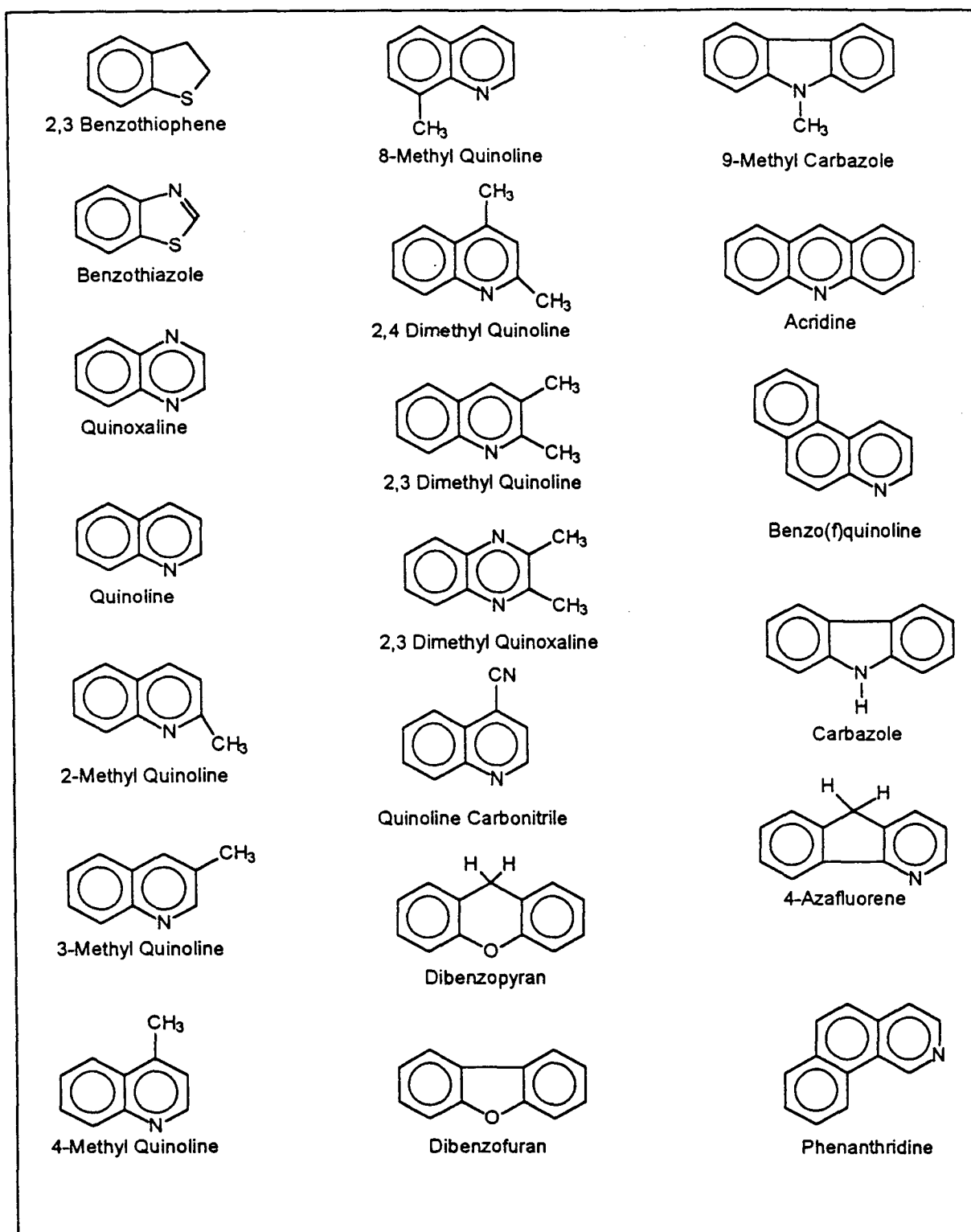
Figure 1. N-, O-, and S- heterocycles examined in this work.

For example, O- and S- heterocycles receive only passing mention in advanced texts (e.g., Klaassen et al. 1986), and there are few synoptic toxicity data (e.g., MicroTox^{tm} results) in the available literature (Lui and Dutka 1988). Of all the common NOSH compounds, the toxicology of the N-heterocycles has received the most attention. In single compound assays, a number of N-heterocycles, including quinoline, all possible C_1-quinolines, carbazole, various benzacridine isomers, dibenzo(a,h)acridine, were mutagenic and tumorigenic in the Ames/*Salmonella* assay and various mammalian test systems, respectively (Krone et al. 1986; Haugen et al., 1982; Lehr and Jerina 1983). This is different from the trend of genotoxicity observed in low and intermediate molecular weight PAHs with the same ring structures (Cavalieri and Rogan 1984; Lehr and Jerina 1983; Philips 1983). Thus, PAHs of 2 and 3 fused rings (*i.e.*, naphthalene, fluorene) are not mutagens in the Ames *Salmonella* assay or carcinogens in mammalian test systems, while the analogous NOSH compounds (*i.e.*, quinoline, carbazole) display mutagenic and/or carcinogenic activity in these systems (Krone et al. 1986; Philips 1983).

In addition to *in vitro* assays, N-heterocycles and PAHs from contaminated sediments have been correlated to extract mutagenicity (Malins et al. 1985), and neoplasia and proliferative disorders in exposed benthic fish (Roubal and Malins 1985). Further, analyses of coal-fired power plant particulates showed that the "most mutagenic" and "bioactive" fraction was the polar fraction containing primarily N-heterocycles and PAH amines (EPRI 1985). Recent studies (Catallo et al. 1990a, 1992a, 1994) have shown acute ultrastructural and bioelectrochemical effects of N-heterocycles and their oxidation products in bioassays using prokaryotic and eukaryotic model cells. Catalytic biomembranes and electron transport centers were disrupted either through changes in metal cation transport processes or direct electrochemical interaction with biomolecules. In other experiments, Ho et al. (1984) showed that dione oxidation products of benzo(*g*)isoquinoline and acridine caused birth defects in insect assays. It is known that early developmental stages of larvae and embryos are ordered by concerted membrane interactions (facilitated solute transport, invagination, induction) and second messenger cascades involving electron transport and cytoplasmic chemical reactions. Toxicants interfering with the timely progress of these events or the evolution of specific products will be embryotoxic and teratogenic, as observed for some NOSHs and their transformation products (Walton and Mill 1988; Ho et al. 1984).

In order to evaluate the environmental fates and effects of pollutant mixtures from various human activities, it is necessary to understand something about the chemistry, toxicology, and persistence of representative chemicals from all major fractions in the parent mixture. NOSH compounds are widely distributed in

natural and synthetic crude oils, coal chemicals, petroleum products, and pyrogenic mixtures (urban particulates, residues from in situ burns of spilled oils), but their environmental chemistry and toxicology have not been studied adequately. The purpose of this work was to take a few steps toward more complete understanding of the fates and significance of representative NOSHs in estuarine sediments. Specifically, the principle objectives of this 24 month project were:

1) To examine the biological and chemical transformations of a complex mixture of N-, O-, and S- heterocyclic compounds (NOSHs) in three marine sediments under different redox conditions in laboratory microcosms. To provide data on the effects of sediment type and electrochemical conditions (e.g., redox potential or Eh) on relative degradation rates of individual NOSH compounds in the mixture.

2) To determine chemical changes in NOSHs during degradation/transformation and estimate related changes in availability and toxicity of transformation products.

3) To attempt to identify major NOSH transformation products using chromatography and mass spectrometry. To synthesize and use deuterated NOSH tracers in these studies for conclusive identification of major stable transformation products.

4) To identify major synoptic changes in sediment microbial communities upon exposure to NOSHs.

5) To evaluate physicochemical and biological factors controlling NOSH fates in marine sediments and possible remediation approaches for NOSH-contaminated ecosystems.

The ultimate objective was to provide further methods development and quantitative data on the fates of toxic polar chemicals in sediments with different physicochemical properties. These data should be applicable to continuing basic and applied biodeterioration research, and hazard/impact evaluation with respect to energy development and waste disposal in marine environments (Cairns 1980; Blumer 1975).

MATERIALS AND METHODS

Reagents and Stock Solutions

Standard NOSH compounds for use in the current study (Figure 1) included quinoline, a series of C_1- and C_2- alkyl quinolines, quinoxaline, 2,3-dimethylquinoxaline, quinoline carbonitrile, 2,3-benzothiophene, benzothiazole, 4-azafluorene, acridine, benzo(f)quinoline, phenanthridine, carbazole, 9-methylcarbazole, dibenzopyran, and dibenzofuran from commercial sources (Aldrich, St. Louis, MO; Sigma, St. Louis; and Pfaltz and Bauer, Waterbury, CT). A coal carbon black (i.e., "anthracene oil") containing PAHs and NOSHs was used as a standard complex mixture for use in evaluating the the degradative abilities and specificity of microbial communities isolated from sediment microcosms (below). A concentrated mixture of the NOSH standards was made up in acetone and used to spike the sediments in the microcosms. Acetone was the carrier solvent in all microcosm experiments. Dimethylsulfoxide (DMSO) was used as the extraction solvent and/or carrier in the toxicity assays, including MicroTox cytotoxicity and *Salmonella typhimurium* mutagenicity assays. Sediment extractions, GC, and GC-MS applications were conducted using dry, ultrapure dichloromethane (DCM) as the solvent. In what follows, total and individual NOSH concentrations will be given in parts per million (ppm; *i.e.*, µg/g) unless otherwise indicated. All solvents were of ultrapure grade, and preparative reagents were of at least analytical reagent grade.

Sediment Microcosms

Three bulk sediment-water samples were collected from sites in the Bay St. Louis estuary (MS). Based on visual estimates, the sediments collected were: a) a fine textured sediment of high clay content typical of quiescent depositional environments, b) a coarser grained silt, usually observed in mixed or occasionally turbulent zones and, c) a sand, typical of high energy environments (river bars, beaches). These were returned to the laboratory and sieved to remove large detrital materials, solids, and sediment particles outside the size ranges of interest. Sediment size distributions were determined using a standard hydrometer method (Catallo and Gambrell, 1987). Although the sediments were mixtures of particles with different diameters (i.e., clay < 2 µm, silt 2 - 16 µm, and sand 16 - 2000 µm), in what follows the three sediments will be identified as "clay" "silt" and "sand". This is for convenience of presentation and is not meant to suggest that the sediments were comprised of only one size range. Thus, the "clay" sediments had the highest proportion of clay sized particles (and the highest total surface area) followed by the "silt" and then the "sand" (q.v., Results and Discussion). The sediments were added to estuarine water and

sterile artificial seawater (Instant Ocean; 15 g/L) at ratios on the order of 1:8 sediment:water (w/w). Dried, ground *Spartina alterniflora* plant matter was added to each sediment at a level of 5% (w/w, based on dry weight of sediment). "Killed controls" were identical sediment-water slurries in which biological activity was terminated by extended autoclaving.

Each of the sediments was added to a controlled Eh microcosm (Fig. 2A) modified for organic chemical work from prototypes described elsewhere (Patrick et al. 1973). The microcosms were fabricated by a glassblower to be vacuum tight with junctions joined via luer fittings and double seated teflon o-rings. Fugative gases were passed through a series of liquid and solid phase (silica bonded octadecyl, Aldrich, St. Louis MO) gas traps (Adams et al. 1982) and then vented to a fume hood. The sediment-water system in each microcosm was adjusted to desired pH (7.5 - 8.0) with 1 N acid or base, and brought to desired Eh range through constant stirring and intermittent bubbling of air (for oxidized, aerobic conditions) or nitrogen (for reducing, methanogenic conditions) (Fig. 2B). In general, the flooding of sediments is accompanied by rapid depletion of dissolved oxygen by microbial respiration and mobile chemical reductants (Ponnamperumma, 1972). In the absence of oxygen, microbial and chemical reductions deplete other electron acceptors (NO_3^-, Mn^{4+}, Fe^{3+}, SO_4^{2-}, CO_2) giving rise to reduced sediment electrochemical conditions (Fig. 3). By balancing the introduction of air and nitrogen to stirred sediments in these microcosms using a first order feedback mechanism (Fig. 2B), various Eh ranges can be established and maintained to simulate conditions found in deep and surface sediments, as well as sediments that are periodically flooded and drained as in many wetlands.

After desired Eh levels of < -250 mV (strongly reducing) and +450 (well oxidized) mV vs. the saturated calomel electrode (SCE) were established for each sediment, the system was equilibrated (poised) for seven days. At this point, sediment samples were taken and extracted/analyzed for NOSHs and possible interfering compounds (below). These data were used to characterize the "clean" (baseline) sediments prior to NOSH additions. Next, aliquots of a NOSH complex mixture (50 ppm of each compound) was added slowly to each sediment followed by mixing for 24 h. The first sediments to be extracted for NOSHs were collected immediately after this 24 h equilibration.

The purpose of the stirred Eh/pH microcosms was to maintain relatively homogeneous redox and pH conditions within the bulk phase of the sediment-water system. Stirring is used because sediments left standing under flooded conditions spontaneously develop Eh gradients and it is necessary to minimize this in order to evaluate the significance of Eh to NOSH degradation rates and pathways. In practice, Eh was monitored *in situ* using

6

A

1. Gas (air or N$_2$) inlet; 2. Pt working electrode (2 per microcosm); 3. Saturated calomel reference electrode; 4. Agar/KCl salt bridge; 5. Thermometer; 6. Solid phase and liquid volatile organic traps; 7. Combination pH electrode; 8. Teflon stir bar.

B
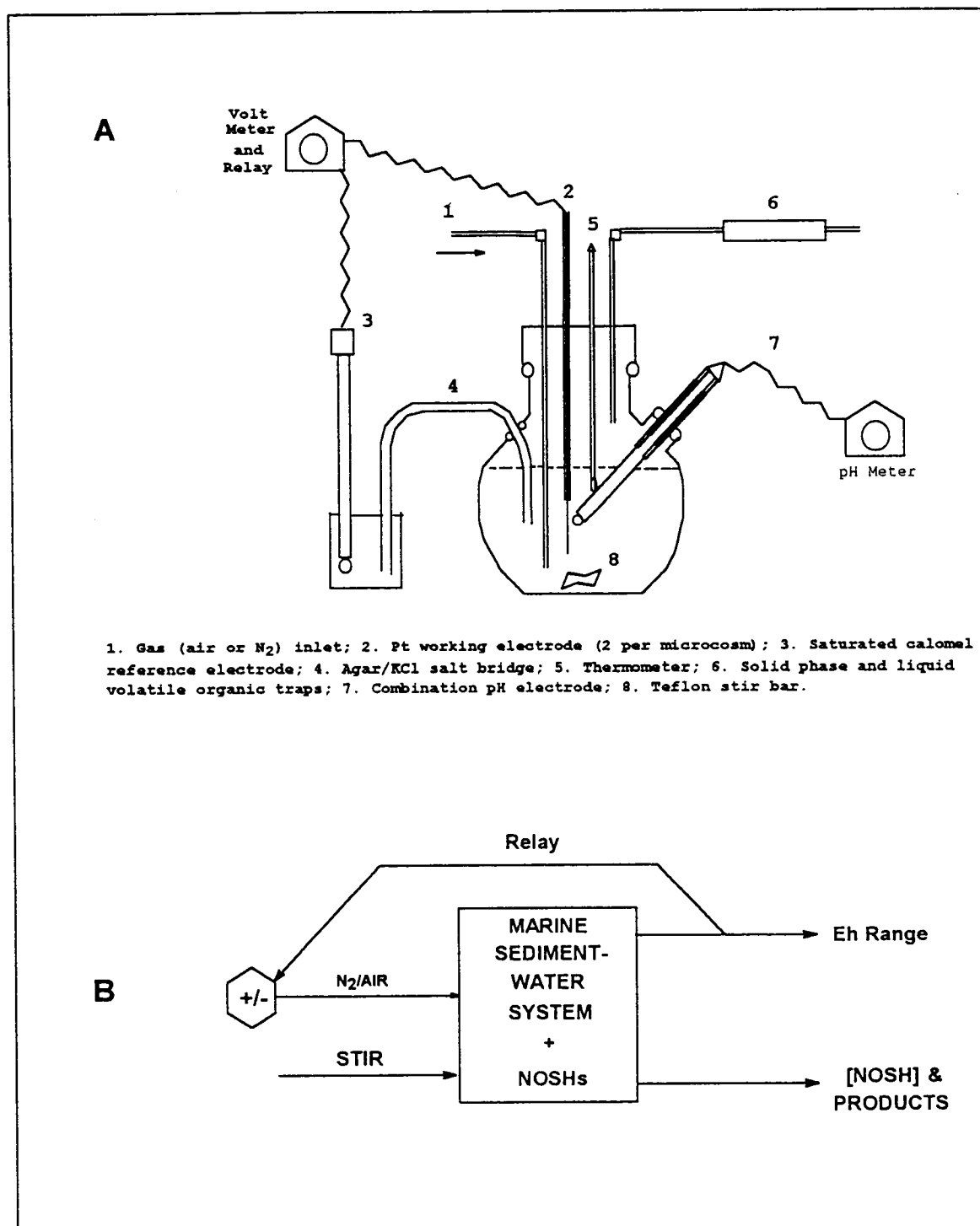
Figure 2. A. Schematic diagram of the controlled Eh microcosm. B. Feedback scheme for the controlled Eh microcosm.

NET REACTION $\qquad$ POTENTIAL vs. SCE

$$O_2 \longrightarrow H_2O \qquad\qquad +600\,mV$$

$$NO_3^- \longrightarrow N_2 + N_xO_y + NH_3/NH_4^+ \qquad +350\,mV$$

$$Mn_s^{4(3)+} \longrightarrow Mn_{aq}^{2+} \qquad\qquad +100\,mV$$

$$Fe^{3+} \longrightarrow Fe^{2+} \qquad\qquad -150\,mV$$

$$SO_3^{3-} \longrightarrow S^{2-} + HS^- + H_2S \qquad -300\,mV$$

$$CO_2 \longrightarrow CH_4 \qquad\qquad -425\,mV$$

$$PO_4^{3-} \longrightarrow PH_3 \quad \text{(Postulated)} \qquad -400\,mV$$

Figure 3. Prominent biogeochemical redox couples observed in estuarine
and wetland sediments.

8

several Pt wire electrode *vs.* a saturated calomel reference electrode (SCE) connected to a multimeter (Fig. 2A). If the desired Eh range was exceeded, the multimeter activated a feedback mechanism that activated/deactivated compressed gas bubbling (air or N_2) until the Eh was returned to the predetermined range (Fig. 2B). The microcosms were maintained for 15 weeks, with sampling at biweekly intervals.

After degradation data were collected from the controlled Eh microcosms for each sediment-water system, degradation of the NOSHs was examined in the three sediments under quiescent conditions more closely approximating a natural environment. The oxidized or reduced conditions were established by adding 5% *Spartina* matter to 1:3 (w/w) sediment:water followed by gas sparging and stirring as above. This was followed by addition of the NOSH compounds and mixing to achieve a homogeneous distribution. The sediment slurries then were added to solvent-clean sealed glass and teflon reactors (c. 40 g wet weight per reactor) and covered with sterile seawater (salinity 15 parts per thousand). The reduced microcosms were maintained under Ar and N_2 in sealed atmospheric glove bags, while the oxidized systems were exposed to a normal atmosphere. All microcosms were opened briefly and shaken manually twice per week so that the development of redox gradients in the system could be minimized. Randomized samples and replicates were collected and analyzed for NOSHs and their degradation products at biweekly intervals over a 23 week period.

Extraction and Analysis of NOSHs
    Aliquots (10 - 100 mL) of slurry from the controlled Eh/pH sediment microcosms were loaded into glass liquid-liquid extractors and extracted for 24 with DCM. The organic phase was dried with anhydrous Na_2SO_4 followed by volume reduction using Kuderna Danish (K-D) concentrators at 80 $^\circ$C. Sediments from the unstirred microcoms were prepared by adding the entire contents of randomly selected reactors and duplicates to pre-rinsed soxhlet nitrocellulose extraction thimbles with enough anhydrous Na_2SO_4 to remove water. The sediments were soxhlet extracted for 36h in DCM, followed by K-D volume reduction. The solid and liquid phase gas traps also were extracted with DCM followed by chemical drying and volume adjustment. NOSH recoveries were estimated by adding known amounts of a surrogate standard (3-methylisoquinoline) to the matrix prior to the DCM extraction. Percent recovery was determined as:

$$\%Recovery = \mu g\ Surr_{(extract)}/\mu g\ Surr_{(spike)} * 100;$$

or the ratio of solvent-recovered surrogate mass measured at the GC detector to known mass of surrogate, which was added to the sediments prior to extraction.

The resulting dried, volume adjusted organic extracts from these extractions were analyzed using gas chromatography (GC) with flame ionization detection (FID) or GC-mass spectrometry (GC-MS). Aliquots of the samples were dried and weighed to determine NOSH concentration on a dry weight sediment basis. Recovery corrected concentrations for target NOSHs were used to construct time course transformation profiles. The NOSH concentrations at each time were determined by referencing of extract data (integrals of peaks at appropriate retention times, Rt) to external five point calibration curves for each compound. Instrument calibration was checked by injection of NOSH standard mixtures at concentrations near the middle of the linear range of the calibration curves (e.g., 50 ppm). As a matter of routine, blanks and calibration standards were run after every third microcosm sample (i.e., for every three consecutive samples were run, an extraction blank and calibration standard were analyzed to check calibration and determine the presence of contaminants). New calibration files were constructed in cases where concentrations of standards differed from expected values by > 15%. Reduction in analyte peak intervals over time was taken as evidence of NOSH transformation while the appearance of novel peaks in extract chromatograms was an indication of degradation products, which subsequently were characterized using GC-MS. The following specifications applied to GC and GC-MS analyses:

GC: Hewlett Packard Model 5890 or Shimadzu GC-17A gas chromatographs, AOC 14 autosampler with Allometrics (Baton Rouge, LA) 12 x 32 mm screw thread sample vials, DB-5MS megabore (30 m; 0.53 mm id; 1.5 μm film) columns (J&W Scientific, Folsom, CA). Injector temp. = 250 °C, splitless, temperature program 55 °C (5 - 10 min), ramp 2 - 4 °C/min to 220 °C, final (5 - 20 min); sampling rate 4 Hz. **GC-MS**: Hewlett Packard 5890 GC with a 5970 MSD; DB-5 capillary column (30 m; 0.25 mm id; 1 μm film); injector 250 °C; temperature program 55 °C (4 min) ramp 2 - 4 °C/min to 250 °C (20 min); sampling rate 4 Hz and mass range 60 - 275 in the full scan mode. Product identification was performed using interpretation of mass spectra based on chromatographic data, molecular ions, isotopic structures, and logical fragment losses (McLafferty, 1980). Mass spectra were considered acceptable if there was a signal:noise ratio of > 3:1 for the base peak of interest, and minimal background interference with respect to isotopic clusters. In general, mass intensities < 20,000 were not considered unless background (noise) signals were insignificant or could be removed by digital background subtraction routines.

In general, GC-MS was used to confirm results obtained using GC, for characterization of NOSH degradation products, and for deuterated tracer/pathway studies discussed below. The NOSH degradation products in the sediment extracts were identified using interpretation of spectra and computer searches of the

National Bureau of Standards and Wiley data bases of organic compound mass spectra. Also used were reference spectra generated using compiunds synthesized in the laboratory, fractionated coal chemical and petroleum mixtures, and condensates from pyrolysis of petroleum and biogenic mixtures.

Toxicity Evaluation
        Based on the available literature, NOSH compounds of 2 - 4 rings generally are toxic to aquatic organisms at concentrations above 1 ppm in chronic exposures. The acute LC_{50} range for quinoline in phyto- and zooplankton is 50 - 140 ppm, and for vertebrates is 5 - 50 ppm (Lui and Dutka 1987).
        In the current work, the toxicity of selected individual NOSHs, a NOSH mixture consisting of the 19 NOSHs added to the sediment microcosms, and extracts from the sediments and water of the controlled Eh microcosms was monitored using the MicroTox[tm] assay (Microbics Corp. Carlsbad CA). Water samples and dilutions thereof were analyzed directly while sediments were extracted in DMSO with ultrasonic treatment (40 min) followed by 0.45 µm nitrocellulose membrane filtration. The protocols for this assay are extensive and will not be detailed here. Basically, the assay relies on progressive quenching of bioluminescence in *Photobacterium phosphoreum* by increasing doses of toxic chemicals. The "EC-50" values (concentration of toxicant required to reduce luminescence by 50% relative to solvent controls) reported in the results were computed from the linear regression of dose vs. luminenscence intensity over a range of exposure concentrations. The assay is designed for rapid comparative toxicity evaluation, but allows for no mechanistic interpretations.
        Mutagenicity of selected individual and mixed NOSHs was determined using the Ames mutagenicity assay (Maron and Ames, 1983). This assay measures the reversion of auxotrophic histidine/biotin(-) mutants of *Salmonella typhimurium* to the wild type by chemical agents that cause DNA damage. Strains designed for detection of frameshift mutations (TA98), base-pair substitutions (TA100) and oxidative damage and DNA strand cross linking (TA 102 and TA104) were used in assays of NOSH compounds that have not been examined previously. Both direct acting and enzymatically activated mutagenesis was examined for each compound and mixture in these assays. In practice, the tester strains were exposed to NOSHs and mixtures in DMSO with and without enzyme preparations (S9) derived from pre-induced rat liver homogenates (Maron and Ames, 1983). The purpose of the S9 mix is to mimic the activity of redox enzymes (mainly cytochrome P-450 and related systems) found in eukaryotes (Ortiz de Montellano, 1986). Its reactions include the generation of electrophilic diol epoxides in certain PAHs, reduction of nitro groups, and disproportionation of redox active centers followed

by generation of radicals or reactive oxygen species (e.g., peroxides) (Ortiz de Montellano 1986; Lehr and Jerina 1983). Thus, both direct-acting (i.e., not requiring enzymatic action to be mutagenic) and "promutagen" (i.e., requiring enzymatic action) mechanisms were evaluated for the NOSHs using these approaches. Individual NOSH compounds examined in these approaches were quinoxaline, 2,3-dimethylquinoxaline, 9-methylcarbazole, benzo(f)quinoline, benzothiophene, and 4-azafluorene. The stock NOSH mixture was comprised of an equimolar mixture of the 19 NOSH compounds examined in the microcosms. Protocols for all assays and interpretations followed the revised standard methods found in Maron and Ames (1983). Compounds were considered mutagenic in these assays if the level of mutation measured as revertant colonies/plate (N=3) exceeded solvent controls by at least a factor of two, with standard deviations within doses < 15%.

Microbiological Apporoaches
       All handling of microbial samples was performed using standard sterile techniques (Collins et al. 1989). Sediments and water from the NOSH microsoms were collected at different time points in the degradation runs described above, and the appropriate anaerobic vs. aerobic conditions were maintained in subsequent transfers and growth of cells. The sediment and water samples were added to broths and solid agars containing trace micronutrients (inorganic N, P, S, Mn, Mg, Ca, Co, Mo, Zn, Cu, Na, Cl, K, Fe, B) and single or multiple organic C sources including NOSH compounds, citrate, nutrient medium (Difco), sterile *Spartina alterniflora* litter and aqueous broth, crude petroleum, and coal carbon black. Microbes showing growth on NOSH compounds (increases in optical density, reduction of iodonitrotetrazolium (Catallo et al. 1990b) and/or the petroleum or carbon black were streaked for single colony isolation. Isolates then were added to restrictive media containing trace inorganic nutrients and single or multiple NOSH compounds as sole carbon sources. Organisms showing growth on NOSHs were maintained for further characterization and NOSH biotreatment studies (below).
       Organisms isolated from the microcosms, and those showing growth on NOSHs as sole carbon sources were characterized using gram stains (to determine gross membrane characteristics) and size/cell morphology was examined using light and scanning electron microscopy. These approaches permitted determination of the number of different cell types in a culture, the cell sizes, and their degree of motility. These and other characteristics (*e.g.*, presence of endospores, color of cultures, growth requirements) were used to infer the probable identities of major cell types. The evolution of specific trace gases from growing cultures can also provide useful information on the biogeochemical behavior of microbial communities. Gas samples

from the headspace of cultures were collected using gas-tight 50 mL syringes, follolwed by analysis using packed column gas chromatography (Shimadzu GC-14A with thermal conductivity and FID detectors). Trace gases analyzed included prominent sulfides (dimethyl sulfide, methyl mercaptan, hydrogen sulfide), carbon species (methane and carbon dioxide), and nitrogen gases (nitrous oxide).

<u>Deuterated Tracer Studies</u>

Elucidation of compound transformation pathways in environmental matrices can be a daunting task. This is particularly true when transformation gives rise to products with significantly altered partitioning characteristics, and subsequent changes in extraction recovery or analytical tractability. Other problems arise from matrix interference (*i.e.*, presence of unresolved or co-eluting background compounds or contaminants) and "mimesis" (different compounds having very similar chromatographic and mass spectral characteristics- *e.g.*, alkylated azaarenes and amino-PAHs of the same molecular weight). Nevertheless, well controlled experimental systems and judicious choice of target compounds and analytical protocols can alleviate these difficulties, making pathway determination possible using common benchtop instrumentation.

The addition of auxilliary approaches such as deuterated tracer methods can enhance pathway studies particularly in cases where degradation products of target chemicals are indistinguishable from naturally occurring organic matter (a problem encountered particularly in sediments and biological samples) or other pollutant chemicals in a complex mixture. Under these conditions, data from deuterated tracer studies frequently can provide unequivocal determination of the origin and identities of resolved compounds. Unfortunately, the commercial availability of deuterated compounds is limited (e.g., there apparently are no NOSHs, alkylated PAHs, or common environmental degradation products available from the specialty chemical suppliers) and compiunds of interest must be synthesized in the laboratory.

In general, deuterium-labelled chemicals are no more toxic than their protiated homologs, and they provide a continuous tracer during degradation experiments: most, if not all, degradation products of deuterated precursors will contain deuterium (including many volatiles). This cannot be said for other stable isotopes (such as ^{13}C) or radioisotopes (C^{14}), unless each carbon in the chemical is labelled. The procedures for exhaustive labeling of even simple chemicals requires *de novo* syntheses that usually are prohibitively labor intensive and costly. There are two major differences between protiated and deuterated chemical homologs that can be exploited for analytical purposes in biodegradation studies:

1) the masses of protiated *vs.* deuterated compounds are different, and fragmentation patterns produced in a mass spectrometer are distinct. Even though deuterated and protiated homologs frequently elute from standard capillary columns simultaneously, the mass spectrometer detects two families of molecular ions and their fragments, each of which are easily identified.

2) The infrared (IR) absorption bands of deuterated compounds are shifted relative to protonated compounds. For example, methane produces a moderately strong absorbance signal at 3048.2 cm^{-1} as measured by an IR spectrometer. The same signal in per deuterated methane (CD_4) would be shifted to 2236.3 cm^{-1}. (NOTE: Of course, deuterons have nuclear spin = 1 and thus are poorly detected in nuclear magnetic resonance spectrometry (NMR). As there is no direct application of NMR to the experiments described in this study, the subject will not be discussed here).

In this work, comparative analyses of isotopic structure for protiated and deuterated homologs given by the mass spectrometer were used to identify metabolites. Characteristic molecular weight (MW) and the patterns molecular ion and fragment isotopic clusters were determined on deuterated vs. protiated NOSH standards synthesized in the laboratory. Occurrence of similar isotopic structures in products with appropriate MW and low mass ion series (i.e., logical neutral losses on ionization in the source of the mass spectrometer) were used to identify products. Disproportionation of completely deuterated compounds causes increased complexity of isotopic structures found by mass spectrometry, and this also can be used for diagnostic purposes. Expected changes in the isotopic structure of deuterated tracers from transformation processes were modelled using digital algorithms written in the C++ programming language (Borland International Inc, Scotts Valley CA) using fundamental relationships provided in McLafferty (1980).

Synthesis of the benzo(f)quinoline-d9 tracer proceeded using stimulated H-D exchange at Pd catalysts at elevated temperature and pressure (Werstuik and Kadai, 1974). Benzothiazole-d3 was deuterated following a novel synthetic protocol: 2-mercaptobenzothizole was synthesized at high temperature and pressure using aniline-d5, carbon disulfide and elemental sulfur followed by recrystallization in ethanol. Deuterobenzothiazole was made by treating the 2-mercaptobenzothiazole with aqueous sodium hydroxide followed by dropwise addition of hydrogen peroxide. After 24 hours of stirring at 30 °C the system was acidified to pH 1 for 4 hours, and then neutralized with sodium bicarbonate. The resulting benzothiazole-d3 was extracted with DCM, dried over Na_2SO_4 and then the solvent was removed via rotary evaporation. Purification of the residue was performed using vacuum distillation.

14

Molecular Modelling

Physical-chemical data on the NOSH compounds such as dipole moment (D), heat of formation, and interatomic bond order were calculated using interactive molecular mechanics algorithms (the MMX force field, Serena Software Inc., Bloomington IN). Also, semi empirical, ab initio molecular orbital calculations were performed using MOPAC self consistent field (SCF) approaches with the MNDO/3, AM1, and PM3 parameterized Hamiltonians (Quantum Chemistry Program Exchange, Chemistry Department, Indiana University, Bloomington, IN). Basically, the MMX algorithms utilize classical force field approaches to minimizing geometries of molecular systems and then estimating minimum configurational energies based on general empirical parameters such as bond distances and angles characteristic of different nucleii (Atkins 1984; Burkert and Allinger, 1982). The MOPAC data were derived from numerical solutions of the time-dependent Schrodinger equation using boundary conditions and parametric constants found empirically or by estimation methods. The SCF approach allows for many-body problems of molecular systems to be reduced to two body approximations (Burkert and Allinger, 1982; Atkins, 1984). In practice, solutions are determined for each electron vs. fixed nuclei and a cloud of all other electrons in the system. Each configuration is solved followed by further iteration and new sets of solutions over the entire molecule of interest. Energy minima for the system are determined, and self-consistency is achieved when successive iterations do not change the total energy of the system (i.e., an energy minimum is reached).

The MMX and MOPAC molecular modelling data were employed to help interpret chromatographic and observed metal complexing behavior of the NOSHs. With respect to chromatographic behavior, a mixture of 19 NOSH compounds was injected to the GC on a standard 30m DB5MS column and exposed to a linear temperature ramp of 4 $^\circ$C/minute after a 4 minute isothermal lock at 70 $^\circ$C. Values of retention time (Rt, minutes) were recorded during the run as the time corresponding to an FID signal maximum (peak) was observed. Other data were assembled including MW, dipole moment (debye) calculated using MOPAC, empirical or calculated log octanol:water partition coefficient (log P) for each NOSH (Leo, et al., 1971), molecular volume ($Å^3$), molar volume (cm^3) total surface area ($Å^2$), total unsaturated surface area, total polar surface area, all calculated using MMX. These data were analyzed using canonical correlation procedures and principle components analysis (PCA) (Davis, 1986).

RESULTS AND DISCUSSION

Chromatographic Behavior of the NOSH Mixture

A representative GC trace of the NOSH standards is shown in Fig. 4. It can be seen that adequate resolution of the compounds was possible using a commercial megabore capillary column, and that isomers (e.g., the methyl quinolines and acridine/phenanthridine/benzo(f)quinoline) were separated. Seperation of NOSHs on capillary columns of smaller diameter and stationary phase film thickness was comparable, albeit with some loss of sensitivity. For unknown reasons, NOSHs from extracted from sometimes showed non-gaussian peak shapes, including tailing and broadening. These anomalies generally were not observed in analyses of NOSH standards, and gave rise to integration problems in chromatograms of some sediment extracts. As a result, some of the variance in measured NOSH concentrations presented below can be attributed to these anomalies. For example, repeated chromatography of extracts with non-gaussian peaks followed by digital integration sometimes yielded data with > 30% coefficient of variation (CV). With standard solutions, CV values typically were < 10%. Detection limits (peaks with signal:noise ratios gretaer than 3) for all NOSHs were 0.5 - 4 ppm using the FID, with lower detection limits observed periodically depending on conditions. Detection limits of the GC-MS in the full scan mode were on the order of 1 ng. Absolute instrument error on automated runs of identical standard mixtures at concentrations in the middle of the linear range was 2 - 9%. Within a given calibration period, peak retention times differed by < 1%.

The relationships between retention times (RT) of the NOSH compounds and various intrinsic chemical factors and molecular modelling estimates were of interest for a number of reasons. In past studies, indeces such as molecular connectivity have been useful for deriving low order equations for predicting Rt of various chemical series (Poole and Poole, 1991). The ability to do this with the NOSH compounds of this study would be useful in in a number of ways, e.g., in determining the likely Rt of trabsformation products.

Results of multiple correlation analyses showed that many of the molecular properties and estimates were highly correlated with RT and each other (Table 1). It is clear from Table 1 that many of the variables interact or can be considered identical (i.e., the off diagonal elements equalling 1.0). As would be expected, molecular weight and log P correlated very well with retention time. The measures of molecular polarity (e.g., polar surface area and dipole moment) were negatively correlated with Rt as expected: the column used had a reversed stationary phase which retains polar compounds more strongly than nonpolar compounds of the same MW. Factor analysis was used to provide eigenvalues of the correlation matrix shown above. The objective

17
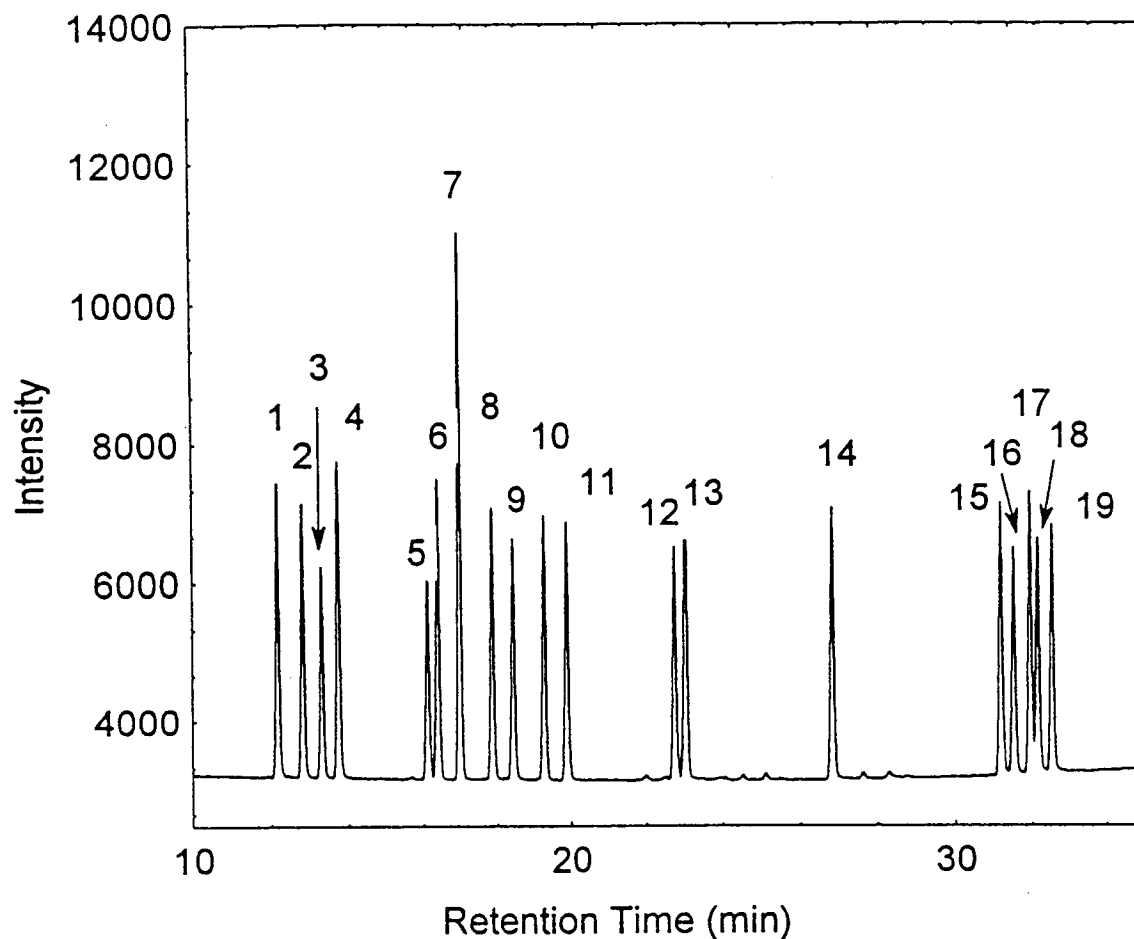
1. Benzothiophene 2. Quinoxaline 3. Benzothiazole
4. Quinoline 5. 2-Methylquinoline 6. 8-Methylquinoline
7. 3-Methylisoquinoline (Surrogate) 8. 3-Methylquinoline
9. 4-Methylquinoline 10. 2,3-Dimethylquinoxaline
11. Quinoline carbonitrile 12. 2,4-Dimethylquinoline
13.Dibenzofuran 14. 4-Azafluorene 15. Dibenzopyran
16. Benzo(f)quinoline 17. Acridine
18. 9-Methylcarbazole 19. Phenanthridine

Figure 4. Typical gas chromatogram of NOSH compounds examined in this work.

Table 1.
Canonical correlation analysis of chromatographic and
molecular properties of the NOSH Compounds

	DIPOLE	MW	LOGP	BP	RT	MVOL	MSAR	TOTSA	SATUR	UNSAT	POLAR
DIPOLE	1.0	-.12	-.03	-.22	-.13	-.02	-.03	-.09	.67	-.33	-.42
MW	-.12	1.0	.94	.91	.97	.90	.90	.94	.19	.89	-.61
LOGP	-.03	.94	1.0	.77	.97	.85	.84	.89	.12	.91	-.53
BP	-.22	.91	.77	1.0	.90	.92	.93	.95	.30	.77	-.71
RT	-.13	.97	.97	.90	1.0	.90	.90	.94	.14	.92	-.58
MVOL	-.02	.90	.85	.92	.90	1.0	1.0	.99	.38	.82	-.80
MSAR	-.03	.90	.84	.93	.90	1.0	1.0	.99	.38	.82	-.79
TOTSA	-.09	.94	.89	.95	.94	.99	.99	1.0	.34	.85	-.76
SATUR	.67	.19	.12	.30	.14	.38	.38	.34	1.0	-.17	-.86
UNSAT	-.33	.89	.91	.77	.92	.82	.82	.85	-.17	1.0	-.33
POLAR	-.42	-.61	-.53	-.71	-.58	-.80	-.79	-.76	-.86	-.33	1.0

MVOL:molar volume, MSAR:molecular surface area, MW:
molecular weight, LOGP: Log octanol:water partition
coefficient, BP: boiling point, RT: retention time, TOTSA,
SATUR, UNSAT, and POLAR are total, saturated, unsaturated
and polar surface areas.

was to isolate a simple underlying structure in the set of
multivariate observations (Rt, MW, etc.) which is expressed as a
pattern of variance and covariances between the variables. Shown
below is a column matrix of the factor scores from this analysis
for each input variable examined, and the multiple linear
regression coefficient for each variable on Rt:

	Factor	Multiple R (Linear Regression)
MW	.981509	0.873
LOG P	.909444	0.788
BP	.948284	0.811
MOLEC VOL	.997182	0.901
MOLAR AREA	.996407	0.899
TOT SURF. AREA	.996864	0.934

The multiple regression and factor analysis showed that the
most significant components were total surface area, molecular
volume, molecular area, molecular weight, boiling point, and log
P. The high factor loadings and corresponding significant
regression coefficients suggest that any of these variables
singly could be used to provide reasonable predictions of NOSH
retention times under the chromatographic conditions described
above using linear equations of the form:

$$MW = 88.477 + 3.15477(Rt);$$

using an empirical value for molecular weight or,

$$TOT\ SURF\ AREA = 133.46 + 2.324\ (Rt);$$

if MMX or other calculation data are available on total molecular
surface area for compounds of interest. Of course, the use of
these equations should be limited to compounds with dipole
moments between 0 and 3.5. Outside this range, bivariate
equations correcting for polar effects on Rt would need to be
incorporated. In this work, the regression equation relating MMX
total surface area to Rt was used to predict or confirm the
retention times of NOSHs that had been oxidized to phenols or
ketones, or those that had been disproportionated and
dearomatized. This approach sometimes indicated that proposed
products be rejected because predicted and observed Rt were not
in agreement. For example, many of the microcosm extracts from
this work had a large peak eluting in the vicinity of the
benzoquinolines that had an apparent base ion with m/z 149. The

m/z 149 ion is characteristic of phthalate esters, which are ubiquitous laboratory contaminants, but no such peak was observed in the numerous extraction blanks analyzed along with the microcosm extracts. Other workers have reported the presence of an oxidized/disproportionated quinoline compound in Siberian crude oil with a molecular ion at m/z 149 (Turov et al. 1987), but no chromatographic or mass spectrometric data were provided, and no standards for the compound in question are commercially
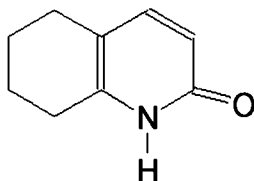
Possible quinoline oxidation/disproportionation
product: m/z 149 (Turov et al. 1987)

available. Using the TOT SURF AREA vs. Rt regression equation above, it was determined that the quinoline product in question (MMX total surface area = 173.6 $\mathring{A}^2$) should elute from the column between 17 and 20 minutes (i.e., around 122 - 134 ^oC). But the m/z 149 compound in the microcosm extracts eluted after 40 minutes. As a result, it was concluded that the m/z 149 compound eluting around 40 minutes probably was a phthalate ester after all, and was regarded as such when it was encountered. Results from deuterated tracer studies of quinoline will be needed to conclusively discount the proposed quinoline product shown above.

In general, data provided by the MOPAC semi-empirical system was less useful on the full spectrum of NOSH compounds studied here than was the MMX force field approach. This was mainly because of limitations of the MNDO/3, AM1, and PM3 methods in handling certain heteroatoms, particularly those characteristic of pyrrole, furan, and pyran. Hence, MOPAC routines frequently failed to converge, had large energy term errors, and failed to achieve self consistent fields. These difficulties and their causes have been discussed by Dewar and Doubleday (1978), Dewar (1983), Dewar et al. (1985) and Burkert and Allinger (1982). On the other hand, the MMX force field was able to provide minimizations and logical structural representations for all the NOSHs studied with minimal computer (CPU) time.

Sediment Particle Size Distribution and NOSH Extraction
The three sediments used in this work were called "sand" "silt" and "clay" for convenience. In reality, each sediment was a mixture of particles from each size range. By definition, sand is characterized by particles with diameters between 16 and 2000

μm, silt 2-16 μm, and clay < 2 μm. Based on hydrometric
measurements, the sediments in this study had percent ratios of
sand:silt:clay sized particles as follows: "sand": 93.2:4.4:2.4;
"silt": 85.2:10.4:4.4; and "clay": 67.2:20.4:12.4. In general,
particle diameter is proportional to total particle surface, but
as diameters decrease to those characteristic of clays, surface
are increases dramatically. For example, clay particles of < 2 μm
in diameter have surface area on the order of 8×10^6 cm^2/g.
Fine sand particles of 0.1 mm i.d. have approximately 227 cm^2/g,
and silt (0.02 - 0.002 mm) 454 cm^2/g (Millar et al., 1986).
Hence, total surface area in pure clay is greater than sand and
silt by four orders of magnitude or more. Using these values and
the particle size distributions given above, approximate total
surface areas of the "sand", "silt" and "clay" sediments used in
this study were determined: sand (192,232 cm^2/g), silt (352,240
cm^2/g), and clay (992,246 cm^2/g). Obviously, percent clay in
each sediment was the main determinant of total surface area. In
the three sediments used here, the ratio of total surface area
was 1.0:1.8:5.2 ("sand": "silt": "clay").

NOSH extraction recoveries and coefficients of variation
(CV) from the controlled Eh/pH microcosms and the unstirred
systems under each redox condition are given in Table 2. These
recoveries were measured using 50 ppm of the 3-methylisoquinoline
surrogate standard.
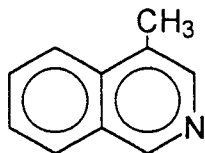
Surrogate Standard: 3-methylisoquinoline

In a very general sense, the recovery data shown in Table 2
suggested that particle surface area and redox status influenced
mean recovery and recovery variance between runs, i.e., surrogate
recoveries from sand and silt tended to be greater than from
clay, and had lower C.V. values. Reducing redox potentials also
seemed to favor higher mean recoveries, but variance was usually
higher than the same sediment under oxidized conditions.
Sorption of organic chemicals to sediment surfaces is a major
cause of analyte losses from environmental samples, so the lower
mean recoveries from clay vs. sand and silt was no surprise
(q.v., surface area estimates above). The apparent redox effect
was counter to expectation, and probable reasons for this
behavior are presented below. It is important to point out that
the trend of decreasing NOSH recovery in clay vs. sand and silt
was minimal because the equilibration time of the surrogate
standard with sediments was short: the surrogate was added to the

Table 2. Recovery of 3-methylisoquinoline surrogate standard
from the stirred and unstirred microcosms

		Stirred Recovery		Unstirred Recovery	
		CV (%)	μ	CV (%)	μ
Sand	(Ox)	17.7	48	20.0	44
Sand	(Red)	18.0	49	22.0	50
Silt	(Ox)	16.0	39	20.5	37
Silt	(Red)	16.0	48	20.2	42
Clay	(Ox)	20.2	44	27.0	36
Clay	(Red)	18.5	48	53.0	41

CV: coefficient of variation (standard deviation/mean) of the
surrogate recovery data; μ is population mean; n= 10 and n= 24 in
stirred and unstirred microcosms, respectively.

sediments immediately prior to extraction while the NOSH analytes
were equilibrated over periods of days to months. Thus, NOSH
analytes in the microcosms were more likely to be tightly
adsorbed to sediment surfaces than the surrogate. The surrogate
data, therefore, provided over estimates of corresponding NOSH
analyte recoveries, especially after many days or weeks of
equilibration in the microcosms.

Mutagenicity and Cytotoxicity Screening of NOSH Standards

Several of the NOSH compounds examined in this study are
documented mutagens in the Ames *Salmonella* Assay and carcinogens
in mammalian assays (see introduction). There apparently are no
data on other possible mutagens used in this work, so these were
examined. A second objective was to evaluate the use of the Ames
assay for monitoring changes in mutagenicity of the NOSH mixture
over time in the sediment microcosms. As mentioned previously,
the assay measures the ability of test chemicals and mixtures to
cause heretable genetic alterations (mutations) of *Salmonella
typhimurium* mutants designed for this purpose. The tester
strains used were selected for their ability to detect specific
kinds of damage likely to be caused by NOSH compounds (Lehr and
Jerina, 1983; Cavalieri and Rogan, 1984). In this work, tester
strains TA 98 and TA 100 were used to detect frameshift and
substitution mutations, while TA 102 and 104 were used to screen
for oxidative mutagens and cross linking agents inclding redox
cycling agents, reactive oxygen species, and organic free
radicals.

Of the single compounds tested, only 9-methyl-carbazole (9-
MC) was found to be mutagenic (Table 3). This compound was
active in TA 100 and TA 104 only after metabolic activation with
liver S9 homogenates. The mutagenic activity of 9-MC was higher
in TA100 which suggested that alkylation followed by excision-
repair errors (substitution) could have been the mechanism of
damage, but specific DNA binding assays would be needed to
examine this possibility. The positive response in TA 104
suggested free radical toxicity either from metabolic products of
9-MC (e.g. 9-MC free radicals), or redox cycling between the 9-MC
and oxygen species in the medium (below). Other work has shown
that 9-H-carbazole can form an N-oxide which can become a
mutagenic N-oxyl radical under appropriate conditions in vivo
(Malins et al., 1985). This species can bind directly to DNA as
a covalent adduct, or cause oxidative damage via superoxide anion
or peroxide. Electrochemical studies in this laboratory showed
that 9-MC underwent 1 and 2 electron oxidation and reduction
reacetions in pH 7.4 buffered saline at potentials found in vivo
and in the sediment microcosms and in cells (Fig. 5). Analysis
of electrolysis products generated at these potentials suggested
free radical mechanisms giving rise to 9-MC dimers and possibly

24

Table 3. Summary of NOSH mutagenicity screening

TESTER STRAIN:	TA98	TA98 (+S9)	TA100	TA100 (+S9)	TA102	TA102 (+S9)	TA104	TA104 (+S9)
DOSE								
(Quinoxaline)								
1MG	23	26	69	71	234	222	207	193
100UG	22	29	73	75	221	225	223	233
10UG	25	25	77	68	213	234	234	235
1UG	27	30	75	79	223	235	237	219
CONTROL	16	27	80	74	205	200	248	204

CONCLUSION: No significant activity at any dose in any strain.

(2,3-Dimethylquinoxaline)								
1MG	19	15	67	62	97	6	117	113
100mg	14	20	101	88	177	123	210	188
10mg	16	18	77	92	176	120	234	182
1mg	17	22	88	77	173	115	236	190
CONTROL	16	16	85	65	191	138	233	186

CONCLUSION: No significant activity at any dose in any strain. Toxicity evident in higher doses.

(9-Methylcarbazole)								
1mg	8	21	14	29	93	62	80	64
100mg	14	17	62	274*	157	151	222	390
10mg	21	16	106	371*	203	170	297	615*
1mg	20	17	105	74	201	150	322	293
CONTROL	15	13	108	65	172	136	307	275

CONCLUSION: Mutagenicity evident in TA100(+S9) and TA 104(+S9). Toxicity observed in higher doses.

(Benzo(f)quinoline)								
1mg	1	4	5	4	2	1	0	2
100mg	13	7	71	60	81	187	109	247
10mg	20	13	84	83	105	216	173	281
1mg	22	8	89	66	117	172	177	257
CONTROL	24	5	83	73	166	140	194	207

CONCLUSION: No mutagenicity observed at any dose in any strain.

(Complex Mixture)								
1 mg	17	50	80	241*	191	282	113	453*
100 mg	22	39	111	136	201	261	204	269
10 mg	28	32	101	116	188	201	206	293
1 mg	23	29	108	113	181	197	203	210
CONTROL	21	36	109	101	173	206	209	211

CONCLUSION: Mutagenicity evident in TA100(+S9) and TA 104(+S9).

(4-Azafluorene)								
1mg	5	7	1	2	96	171	12	162
100mg	22	8	103	74	201	261	204	269
10mg	15	11	97	70	188	201	206	293
1mg	21	10	99	75	188	197	203	210
CONTROL	13	97	69	181	206	209	267	211

CONCLUSION: No mutagenicity observed at any dose in any strain. Toxicity in higher doses.

Data are means of three replicate plates at each dose; standard deviation (s) < 15%; * highly significant increase in reversion rate over solvent controls.
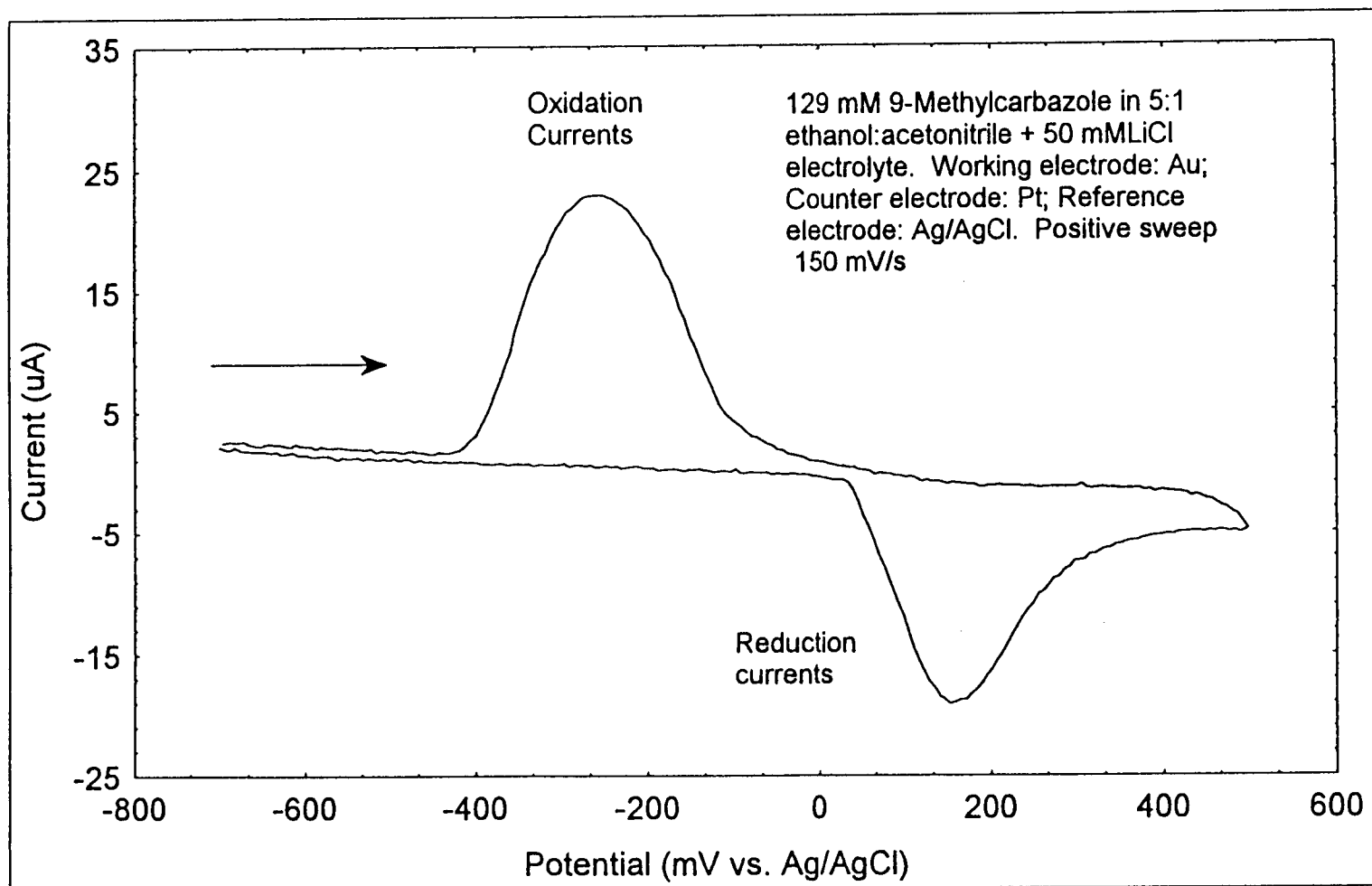
25

Figure 5. Cyclic voltammogram of 9-methylcarbazole.

N-oxides. These electrochemical studies were conducted in deoxygenated physiological saline, and under these conditions organic free radicals are short lived. Hence, dimerization of the 9-MC at electrode surfaces would be expected. Conversely, heterogeneous chemical conditions found in living systems can stabilize free radicals and increase their potential for interacting with various cellular targets including proteins and DNA. For example, the first author has demonstrated that N-heterocyclic mutagens based on phenazine can form stable radicals in nonpolar liquid phases (Catallo et al., 1992b). Hence, redox generated free radicals can be sequestered in nonpolar phases (e.g., lipids) and anaerobic microregions and remain stable for
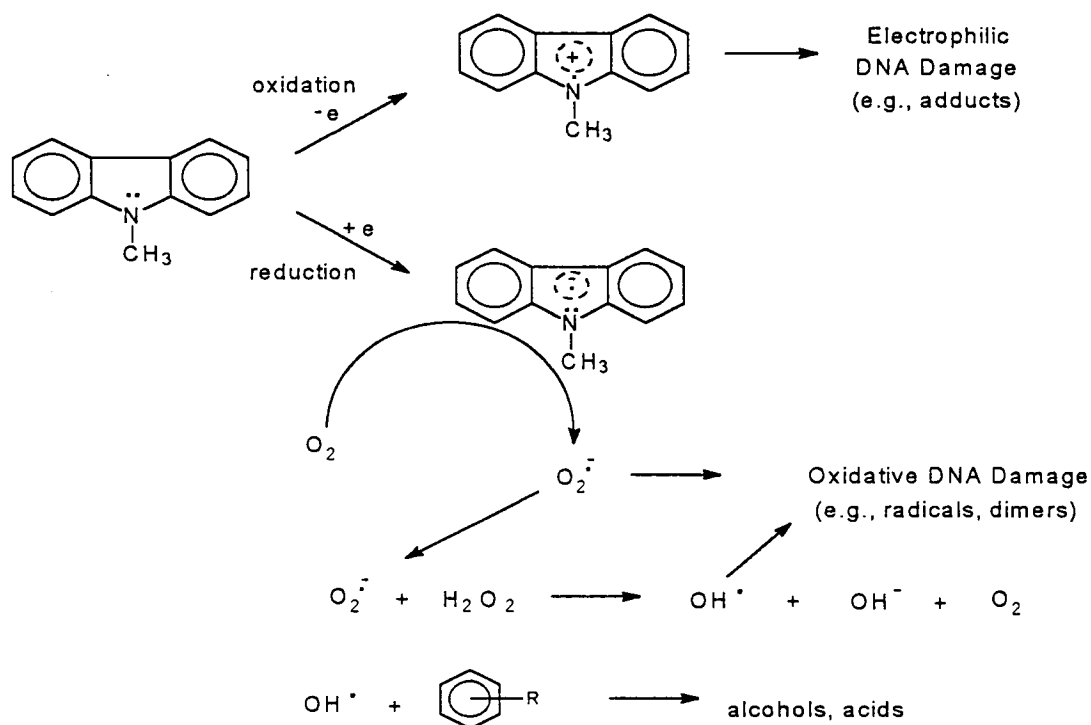
long periods (e.g., several min.). The persistence of free radicals in vivo is thought to be a major cause of biochemical toxicity (Catallo et al., 1992b). As illustrated above, some possible reaction routes involving redox-generated 9-MC free radicals include direct interaction of 1 electron oxidation products (electrophiles) with DNA, and the secondary generation of reactive oxygen species (e.g., superoxide anion) from 1 electron reduction products are shown in the scheme above. Both mechanisms are consistent with the results of the Ames assay shown in Table 3. Further investigation of the toxicity mechanisms and electrochemistry of the alkyl carbazoles with respect to pathways suggested above would be interesting and

relevant to the evaluation of the environmental significance of mixtures containing these chemicals (Frolov and Vanyukova, 1988).

The complex mixture of NOSH compound used in the microcosms showed mild mutagenic activity in strains TA100 and TA104 only after metabolic activation with S9. There was no significant activity in the other strains with or without S9 enzymes. The concentration of the NOSH mixture needed to elicit a minimum mutagenic response (i.e., 2 times above solvent controls) was very high relative to 9-methylcarbazole alone, and this suggested that chemical antagonism occurred in the mixture. For example, 10 µg 9-methylcarbazole was sufficient to elicit a five-fold increase in reversion rate (i.e., mutation) in TA100 with S9. The NOSH mixture, which contained 9-MC and other mutagens such as quinoline, methyl quinolines, 2,4-dimethylquinoline, and 9-H-carbazole elicited only a two-fold increase in TA100 with S9 at the highest dose tried (1 mg of each NOSH compound). Hence, the NOSH complex mixture had a measured level of mutagenic activity two orders of magnitude less than one of its consitituents measured alone (9-MC) in the same tetser strains. Chemical antagonism within mixtures is not uncommon (Austin et al. 1985) and suggests reasons why environmentally mediated alterations of complex mixtures can be significant toxicologically: as weathering, biodegradation, volatilization, and partitioning processes proceed on elements of the mixture, the availability of individual compounds or "fractionated" simple mixtures can increase (cf., Austin et al. 1985). This can correspond to an increase in toxicity and/or mutagenicity relative to the starting mixture (McCann et al. 1975).

The mutagenicity data on the NOSH mixture indicated that the Ames assay was not an acceptable way to monitor mutagenicity changes in the sediments studied here. In order to elicit a positive response from sediment extracts containing the NOSHs, it was necessary to concentrate the extracts by a factor of around 100. Preliminary dosing experiments indicated that biogenic and other materials in the concentrated extracts (e.g., sulfides) were toxic to the tester strains. Toxicity of this kind decreases the number of viable test bacteria in the assay, and dose-mutation relationships cannot be determined with confidence.

As a result of these limitations and the lack of a comparable alternative mutagenicity assay, a quicker, less laborious, and more sensitive cytotoxicity assay (MicroTox) was used for monitoring the toxicity of the microcosm extracts (see below). While not providing a mechanistic account of mutagenic effects of NOSH transformations, the assay was adequate for detecting changes in toxicity of the NOSH mixture at concentrations used in the microcosms and found in extracts.

The MicroTox assay was used to determine the relative toxicity of individual NOSHs and the mixture applied to the microcosms. Unlike the results of the Ames assay, which

indicated antagonism between the NOSHs in the mixture, the MicroTox assay showed a marked synergism in the mixture. Thus, 9-methylcarbazole gave a 5 minute EC_{50} of 315 μg/mL and benzo(f)quinoline had an EC_{50} of 5.4 μg/mL , but the NOSH mixture had an EC_{50} of 0.16μg/mL.

Bulk Properties of the Controlled Eh Microcosms and Batch Vial Microcosms

The controlled Eh-pH microcosms as modified for this work allowed for reasonable control of redox potential and pH within desired ranges for all sediments examined (Fig. 6). In all cases, the oxidized sediments were a characteristic gray color and gave no detectable odor of sulfides, which are anaerobic products of sulfate reduction in marine systems (Fig. 3). As a result of sustained oxidized conditions, films of precipitated iron (III) oxides and oxyhydroxides (red-brown in color) were observed on the electrodes and as films on the glass in the microcosm. Conversely, the reduced sediments were metallic blue to black in color, and sulfides were detected at the gas trap outlets. There was no evidence of precipitated metal films as with the oxidized microcosms, because reducing conditions favor the soluble, divalent forms of Fe and Mn (Fig. 3). In all reduced microcosms, there was evidence of complex sulfur transformations. Sulfur species routinely observed in DCM extracts included elemental sulfur (S8) in the reduced microcosms, while the headspace contained mixtures of hydrogen sulfide and dimethylsulfide (DMS).

In general, the bulk properties of the sand and silt slurries in the stirred microcosms seemed significantly different from the clay microcosms. While the silt and sand slurries behaved as heterogeneous mixtures of solid particles suspended in liquid water, the clay appeared more like a colloidal suspension. This difference also could be seen under a light microscope at 40 X: individual particles of sand and silt could be easily differented from one another and the bulk aqueous phase, while the clays appeared more like gels. At a microphysical level, it is likely that the small particle size and higher total surface area of the clay particles allowed for hydration phenomena to change the bulk characteristics of the system vs. the sand and silt. It is well established that increasing surface area promotes phenomena such as adsorption of hydrophobic chemicals and attachment of microbes. Conversely, processes such as volatilization, degradation, and analyte recovery are decreased by increasing surface area. Decreased volatility of some NOSHs was observed in the clays vs. the sand and silt. For example, extraction and analysis of the gas traps from the controlled Eh microcosms showed that significant amounts (e.g., 70%) of 2,3 benzothiophene was very quickly (24 h) blown out of the sand and silt microcosms (see below). In clays, less than 5% of the total
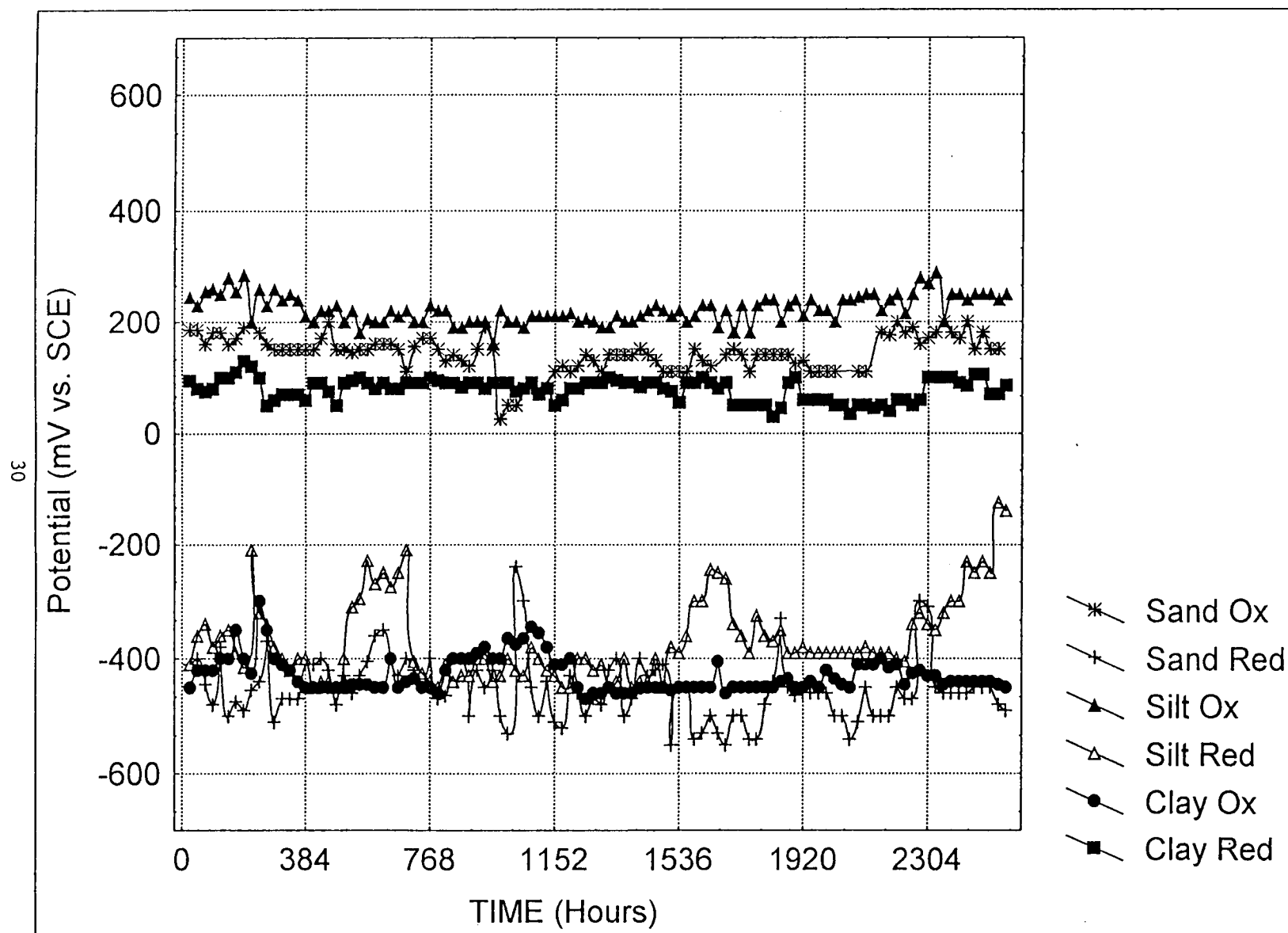
Figure 6. Time series of redox potential (Eh) values measured in the controlled Eh microcosms using Pt electrodes.

2,3-benzothiophene was lost to volatilization over the entire
run, presumably because of rapid sorption on the high available
surface area of the stirred clay particles. The unstirred
microcosms had characteristics similar to the controlled Eh/pH
systems with respect to differences in color, the evolution of
sulfides, and the presence of oxidized iron films in oxidized vs.
reduced treatments. The systems were sealed and did not receive
bubbling of gases or continuous mixing, so the losses of
benzothiophene and other light NOSHs were minimized in all
sediments relative to the controlled Eh microcosms. In spite of
manual shaking and introduction of air every 84 hours, the
oxidized microcosms tended to become mildly reducing,
particularly towards the end of the runs (e.g., 19 - 22 weeks).
The reduced microcosms under Ar/N_2 in glove bags remained
strongly reducing throughout the experiments, with no tendency to
become oxidized with time.

NOSH Fates in Controlled Eh/pH Microcosms
     NOSH concentration-time profiles in the controlled Eh/pH
microcosms are shown in Figures 7 - 9. As mentioned, rapid
volatilization losses were observed for 2,3-benzothiophene in the
sand and silt microcosms, so no transformation rate data could be
determined for that compound in those sediments. The remaining
2,3-benzothiophene was oxidized to sulfoxides and sulfones in the
oxidized systems, as shown by GC-MS product analysis (below).
Much smaller (ca. 1 - 2%) amounts of benzothiazole and quinoline
were volatilized in the early stages of the runs, but this was
constant between microcosms and was not considered significant
with respect to determining relative transformation rates in
situ. Also, recoveries of acridine, carbazole, 9-methyl
carbazole, dibenzopyran and dibenzofuran were consistently poor
in the sand and, to a lesser extent, the silt microcosms. This
was not due to volatilization. Product analysis using GC-MS and
electrochemical studies (Fig. 5) suggested that these compounds
can undergo rapid chemical reactions that alter their phase
partitioning characteristics and limit recoveries. These
reactions included electrochemical transformation to oxidized
products or dimers and protonation of heteroatoms followed by
phase transfer to the aqueous phase as water soluble ion pairs.
Interestingly, in the clay microcoms the chemical reactions of
these compounds and the concomitant formation of altered products
was observed in extracts only after extended incubation (334 h).
This suggested that chemical sequestration of these compounds
occurred in the clays, probably at surfaces, where chemical and
biochemical reactions were minimized (q.v., Parris 1980; Weber et
al. 1993).
     It can be seen from Figure 7 that recovery of most NOSHs in
the oxidized and reduced sand microcosms decreased to low levels
(< 1 ppm) over the experimental period. There was an apparent
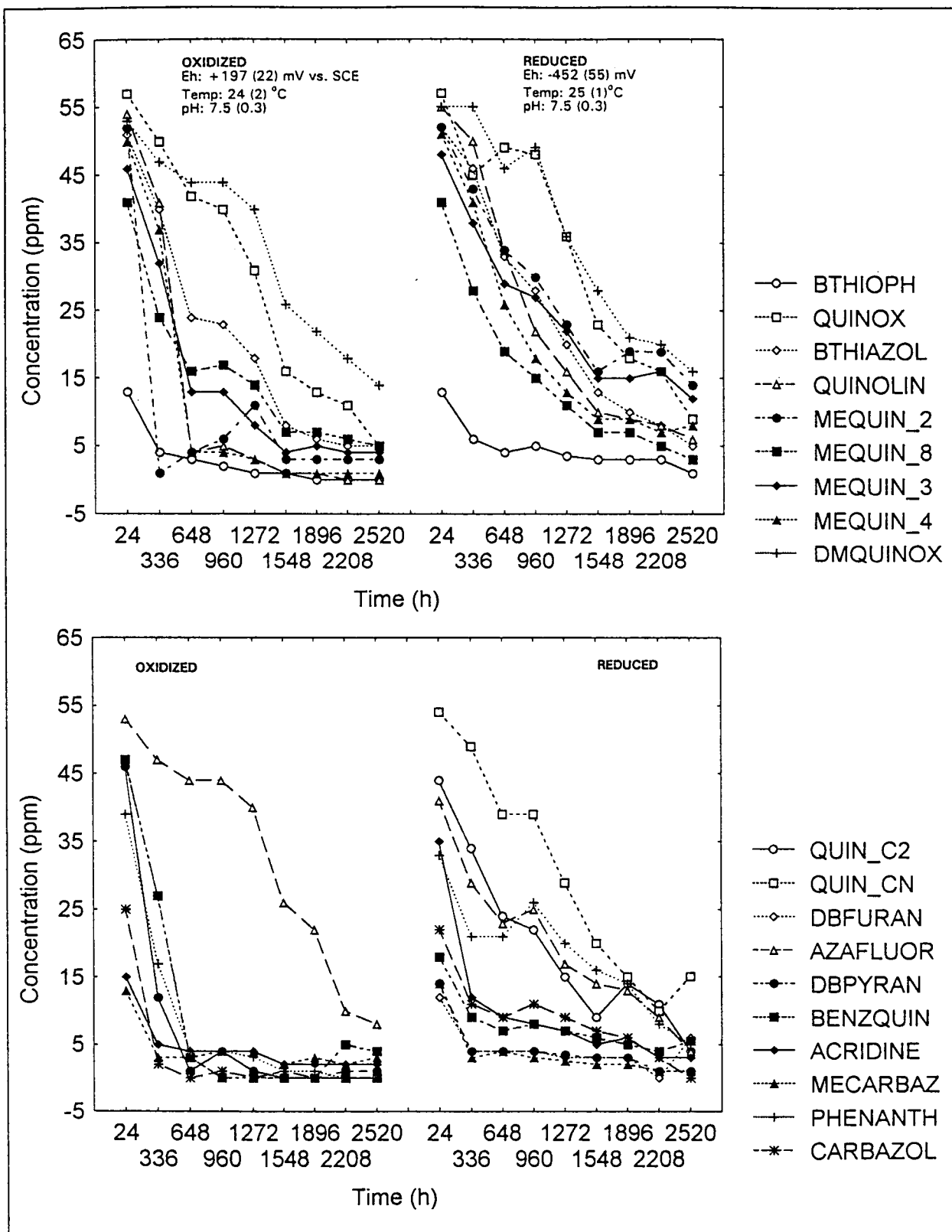redox effect on the transformation rate of the NOSHs in the sand

31

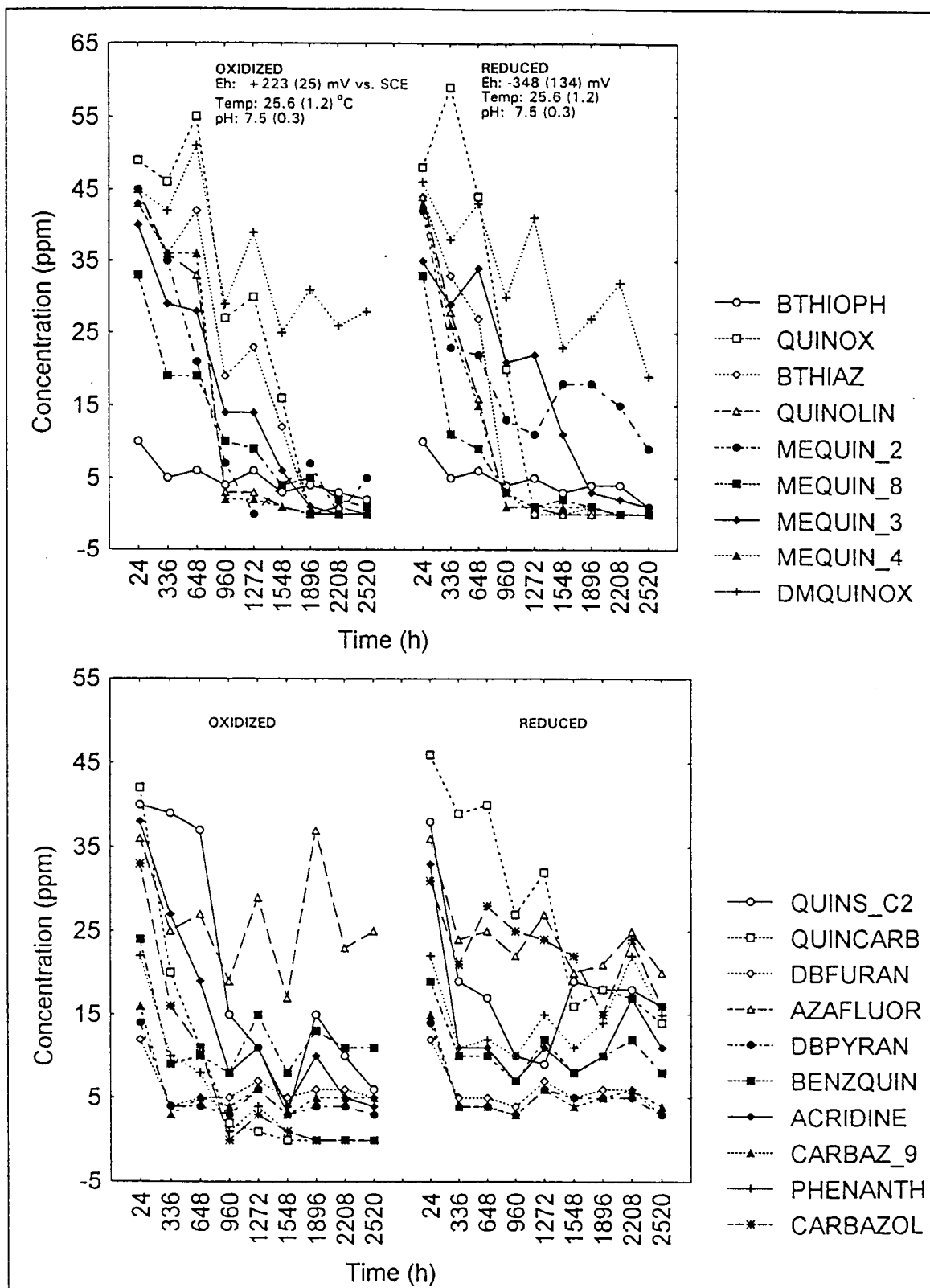Figure 7. NOSH transformation profiles in oxidized and reduced sand.

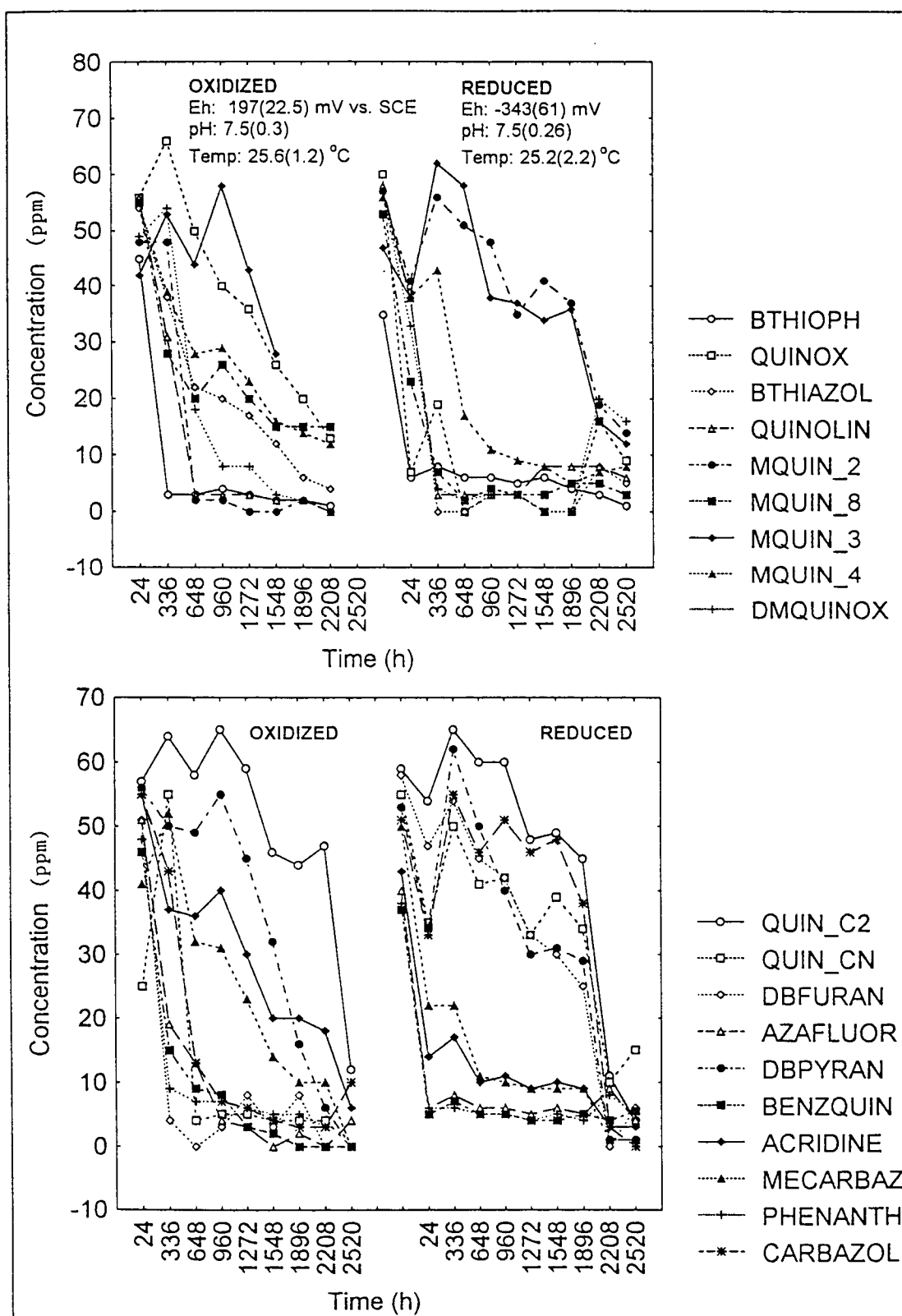Figure 8. NOSH transformation profiles in oxidized and reduced silt.

33

Figure 9. NOSH transformation profiles in oxidized and reduced clay.

34

and silt microcosms: with the exception of quinoxaline, 2,3-dimethylquinoxaline, quinoline carbonitrile, and 4-azafluorene, the NOSHs were removed most rapidly from the oxidized systems than the corresponding reduced system. This effect was particularly pronounced with quinoline, 2-methylquinoline, 3-methylquinoline, phenanthridine, and 2,4-dimethylquinoline. Benzothiazole showed similar disappearance rates under oxidized and reduced conditions.

The relative effects of redox status on NOSH degradation was less apparent in the silt microcosms (Fig. 8) than in the sand. As with the sand, quinoline carbonitrile, 2,3-dimethylquinoxaline and 4-azafluorene were persistent under both redox regimes, showing little difference between them. Unlike the sand, quinoxaline was transformed in the silt, with faster removal observed under reduced conditions. Quinoline, 4-methylquinoline, 8-methylquinoline, and benzothiazole also were transformed at approximately equal rates under both redox conditions, with some a slightly more rapid transformation of 3-methylquinoline, 2-methylquinoline, and carbazole observed under oxidized conditions. As mentioned, recoveries of 9-methylcarbazole, dibenzopyran, acridine, and dibenzofuran were poor at all time points in both oxidized and reduced silt microcosms. The chemical reactivity/recovery problems with these NOSHs made it infeasible to compare results between treatments.

With respect to most compounds examined, transformation in the oxidized sand microcosms proceeded faster than the oxidized silts. Under reduced conditions, however, quinoline, quinoxaline, 4-methylquinoline and 8-methylquinoline, were transformed more rapidly in the silt than the sand. In both cases 2,3-dimethylquinoxaline, quinoline carbonitrile, and 4-azafluorene were degraded slowly relative to quinoline and the alkyl quinolines.

The results obtained in the clay microcosms were different than the sands and silts with respect to recovery of labile NOSHs (e.g., 9-methylcarbazole, dibenzopyran) and the observed transformation profiles of the target analytes (Fig. 9). For example, several of the methyl quinolines were persistant and remained at substantial levels over the entire run in both oxidized and reduced conditions, while quinoxaline and 2,3-dimethylquinoxaline were degraded more rapidly. Unlike the sand and silt microcosms, 2,3-benzothiophene was not sparged from the system and transformation of 9-methylcarbazole and dibenzopyran was not observed until after 336 hours. This suggested that transformation and other processes limiting the recoveries of these NOSHs (e.g., in the sand and silt) probably occurred in the aqueous phase, rather than on sediment surfaces. This was most likely the result of the greater amount of reactive surface in the clay vs. the silt and sands, and the different bulk phase behavior of the former. It is noteworthy in this regard that geochemical data suggest that alkyl carbazoles are stable in fine

35

grained reduced sediments from lacustrine and estuarine systems (Wakeham 1979).

The rate of NOSH removal from these microcosms agree closely with the degradation rates of selected NOSHs in water reported by other workers (Chou and Bohonos, 1979). In the cited work, 10 ppm of benzo(f)quinoline was found to be completely degraded in sewage sludge within 48 h. The same amount of degradation in an estuarine water sample took 35 days. This was very close to the disappearance rate of benzo(f)quinoline observed in the stirred microcosms of the current study. There was further agreement between the two studies with respect to other NOSHs including quinoline, which degraded in estuarine water in 10 - 15 days vs. 27 - 40 days in this work, and benzothiophene, which showed minimal degradation in both studies. These data, and much slower degradation rates measured in the unstirred microcosms (below) indicated that the sediment-water slurries in the controlled Eh/pH microcosms behaved more like an estuarine water sample than a typical sediment. It would seem that processes resulting from stirring and bubbling of these systems increased the importance of aqueous phase reactions relative to what would be seen in an undisturbed, flooded sediment profile.

The typical concentration vs. time curves observed for most of the NOSHs in the controlled Eh microcosms were linear or sigmoidal. This was characterized by an acclimation time of several days-weeks followed by linear decreases in NOSH concentration, and then slower asymptotic approaches to baseline. These kinetics are entirely consistent with those measured for NOSHs in various water samples, and other aromatic hydrocarbons in soils and sediments (q.v. Chou and Bohonos 1979). The acclimation period of the microcosms was accompanied by changes in microbial community structure (below). During the linear and asymptotic phases of the NOSH degradation vs. time profiles, numerous transformation products were identified in the extracts (Fig. 10) using GC-MS. These data showed that a complex suite of transformation reactions occurred in the microcosms. These included a) oxidation of aromatic rings to phenols, ketones, and epoxides, b) disproportionation, saturation and opening of benzylic rings, c) oxidation of alkyl side chains followed by decarboxylation, d) oxidation of heterocyclic sulfur to sulfoxides and sulfones, e) addition reactions (alkylation, glycoaldehyde addition) and, f) β oxidation of opened rings and oxidized side chains. Interestingly, the NOSH transformation product distributions were very similar in oxidized and reduced systems. For example, ketone products of acridine, dibenzopyran, and 4-azafluorene were seen under both redox conditions, albeit after longer incubation times in the clay sediments. Previous work has shown that 4-azafluorene and similar compounds can be chemically oxidized to the corresponding ketones and quinones in rapidly in aqueous media, both of which would be poorly recovered
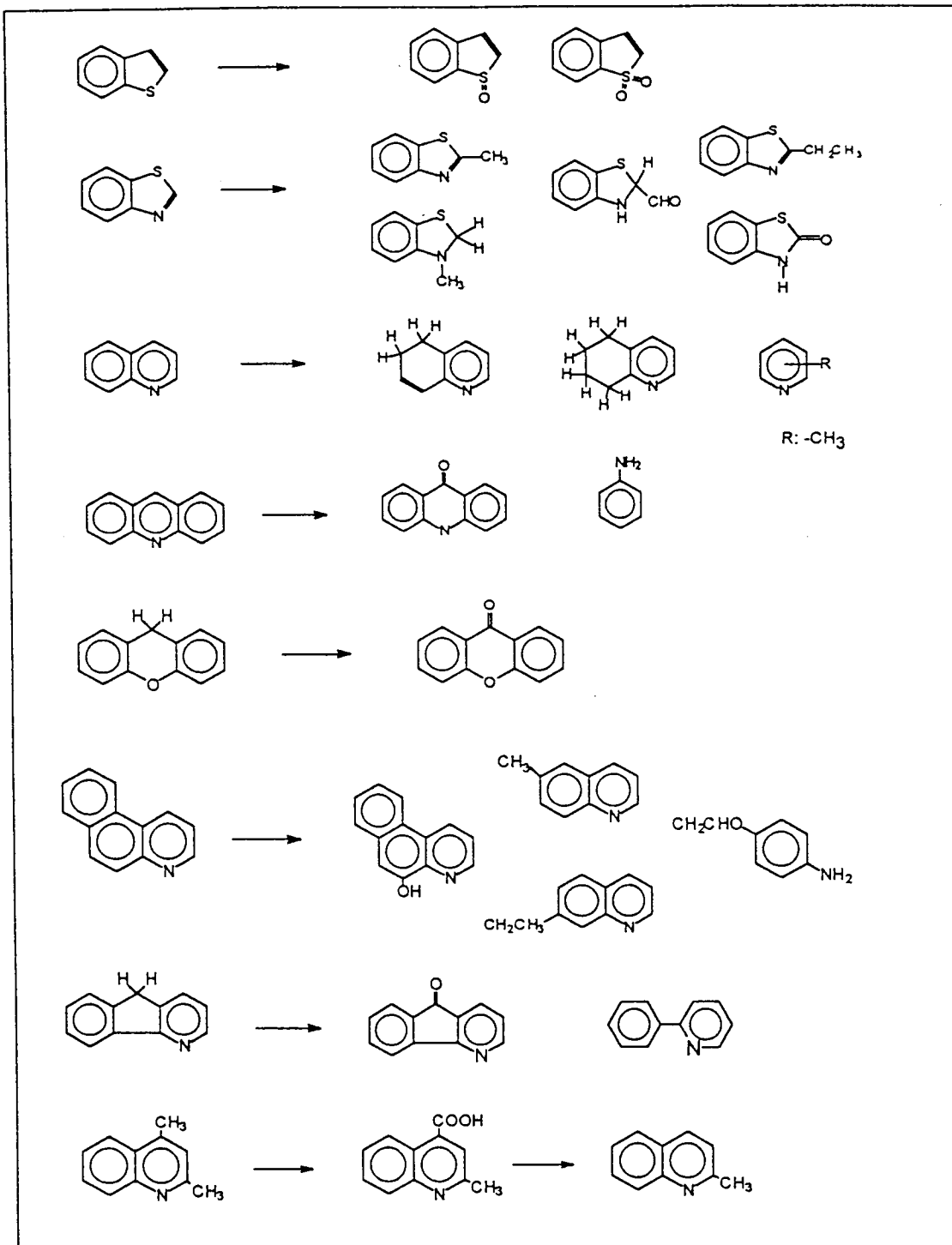
Figure 10. Examples of NOSH transformation products identified in extracts from the controlled Eh and sealed batch vial microcosms using GC-MS.

37

in DCM extracts (Catallo 1989). The 2,3-benzothiophene was oxidized to the 2,3-benzothiophene sulfone which accumulated under oxidized conditions, but thiophenol (C$_6$H$_6$S) seemed favored under reduced conditions. In general, many of the chemical and biological transformation products were oxygenated and more polar and water soluble than the parent NOSH compounds, even in redcued sediments. The partitioning of these materials between polar and nonpolar liquid phases (as with DCM extracts of the aqueous slurries) did not favor recovery and identification using GC or GC-MS. Further, many of the oxygenated NOSH products had very different (typically lower) response factors at the FID and MS detectors vs. the parent NOSH compound. As a result of these problems, and the lack of available standards for the degradation products, mass balance using estimated concentrations of these transformation products would not be appropriate (i.e., existing calibration files would be invalid, and there were no standards available for constructing new ones). As indicated above, 9-methylcarbazole, dibenzopyran, acridine, and dibenzofuran were rapidly altered in the aqueous phases of the sand and silt microcosms. The most frequent products of these compounds were phenol/ketone systems generated at sites containing exchangable (acidic) protons (e.g., para to the heteroatom in the central ring as with dibenzopyran). These were typically observed in the early stages of the sand and silt microcosm runs. As shown (Fig. 5), 9-methylcarbazole can undergo redox reactions well within the range of potentials achieved in these microcosms. This, and the presence of reactive oxidants and reductants in situ probably allowed for rapid transformation or sequestration (e.g., as dimers) of the compound. The significantly greater recovery of these NOSHs in clays vs. silts and sand suggested that rapid redox and other reactions were quenched by the high particle surface area in the former. As said, the silt and sand slurries in these microcosms behaved more like water than sediments with respect to NOSH degradation profiles, but the clays slurries had more sediment character (e.g., slower degradation of many NOSHs, increased sortpion/sequestration of labile compounds, reduced volatilization losses). The significant differences in NOSH behavior between the clay and the other sediments suggested that many chemical and biochemical reactions of interest occurred more rapidly in the aqueous phase than at surface sites on particles. Thus, processes in the stirred sand and silt slurries had much more pronounced aqueous character than the clay, which had a significant surface effect. Further mechanistic work on effect of aqueous vs. solid phase reactions on NOSH fates is called for in light of these observations.

Time Course Toxicity Evaluation of NOSHs in Marine Sediments

As discussed, sensitivity and matrix interference problems precluded the use of the Ames mutagenicity assay for monitoring time course changes in NOSH mixture mutagenicity in the sediment

microcosms. Water and sediment toxicity changes were evaluated
using the MicroTox assay at time points corresponding to the NOSH
analyses (i.e., as shown in Fig. 7 - 9). The time course
toxicity data for water and sediments in each microcosm are given
in Fig. 11 and 12. It was found that sediments were toxic in
this assay even before the addition of NOSHs, and this rendered
much of the sediment data uninterpretable: the sediment extract
toxicity was unaffected by NOSH addition to the system and
changed little throughout the experiments.

On the other hand, water samples from all sediment
microcosms except the reduced clay showed time course toxicity
profiles that generally followed the NOSH degradation profiles.
Prior to NOSH addition, the water from these microcosms elicited
no significant toxicity in the assay relative to buffer controls.
The toxicity increased sharply upon addition of the NOSHs.
Towards the middle of the runs, the water samples showed evidence
of detoxification: there consistently was no difference between
aqueous samples and controls. Water samples from the reduced
clay microcosm, however, were toxic before the NOSHs were added.
The most likely explanation for this is metal and sulfide
toxicity. Nevertheless, the water in this microcosm also became
relatively detoxified in the latter part of the run. The
consistently high toxicity of water samples from the reduced clay
corresponded to the results of chemical analyses: several NOSHs
remained untransformed in this system over virtaully the entire
run.

The aqueous extracts of all but one microcosm behaved
similarly: after an initial period of high toxicity and
subsequent nonlinear variations, the aqueous phase tended to
become nontoxic towards the end of the runs. The nonlinearity of
this function suggested that over time the NOSHs were metabolized
and/or chemically weathered to relatively nontoxic products, but
that toxic intermediates may have evolved in the process. The
presence of transformation products in extracts from these time
periods and the results of tracer studies (below) supported this
interpretation.

Characterization of Microbial Communities
    The time course of NOSH concentrations in the controlled Eh
microcosms was accompanied by changes in indigenous microbial
community structure, as indicated by microscopic examination of
samples, and growth of representative forms in nutrient media.
Prior to the introduction of NOSH compounds to the sediments, the
microbial communities were characertized by diverse assemblages
of bacteria including motile and nonmotile gram(+) and gram(-)
rods, cocci, and filamentous forms. Aerobic samples from clean
sediments contained a range of aerobic and facultatively
anaerobic bacteria and several distinct fungal forms. The
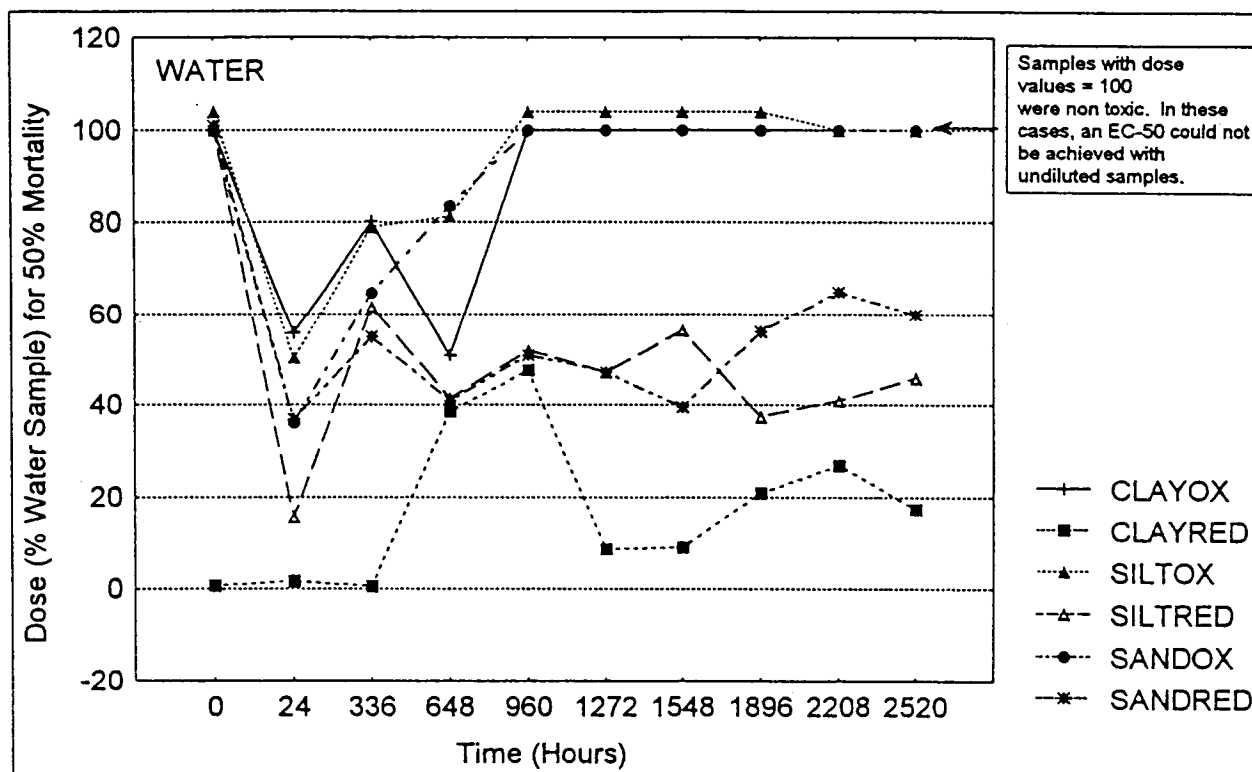bacteria included assortments of gram(-) (e.g., *Psuedomonas sp.*)

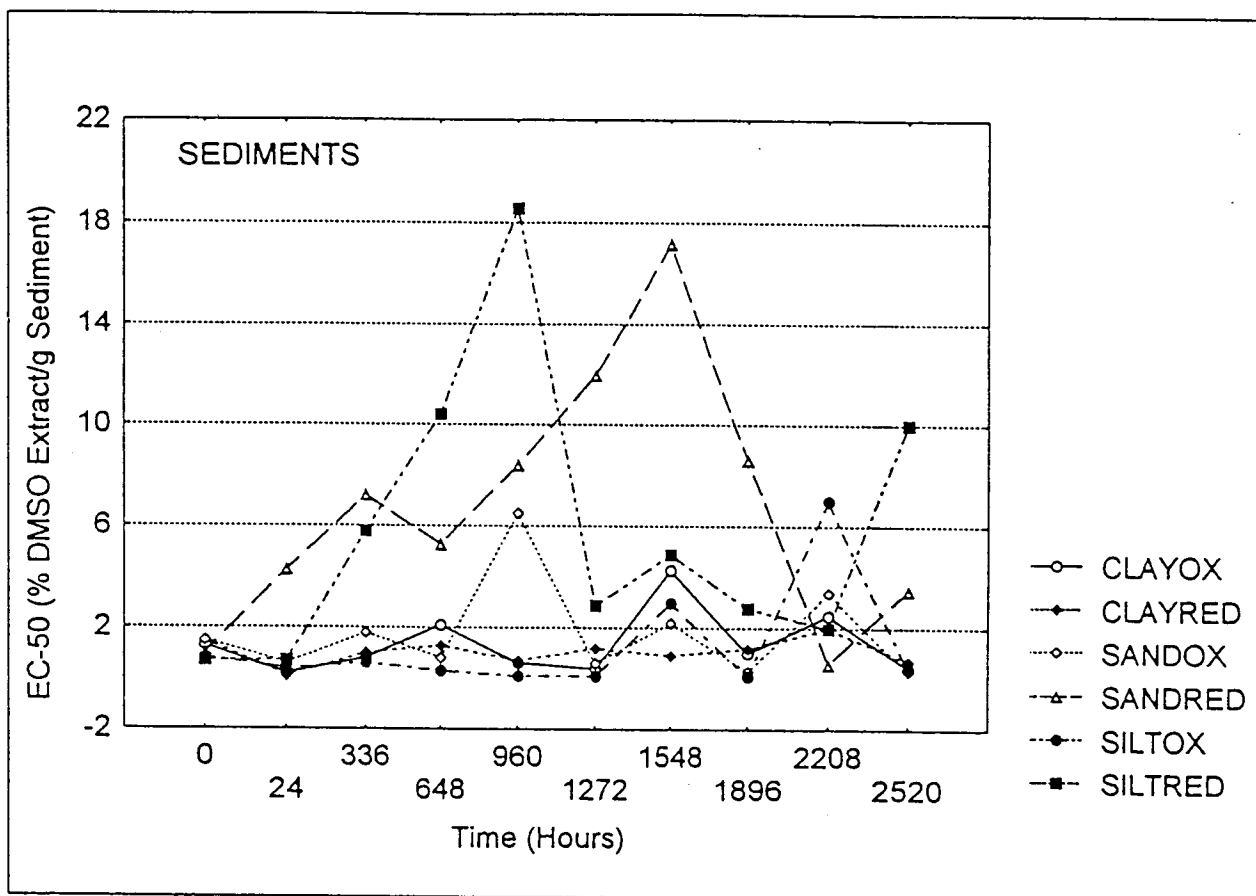Figure 11. Time course toxicity profiles of water samples from the controlled Eh microcosms.

40

Figure 12. Time course toxicity profiles of sediment samples from the controlled Eh microcosms.

41

and gram(+) rods and cocci as well as filamentous species.
Likely identities of prominent species included motile, small (1
- 3 μm x 0.5) gram(-) rods (probably *Thiobacillus sp.*), which
commonly were observed in association with larger numbers of
large (> 16 μm x 0.7 μm), sessile, asporogenous, gram(-) rods
(probably *Desulfomonas sp.*) and flagellated, large (> 16 μm x 0.5
μm), gram(-) rods (probably *Desulfovibrio sp*). At least two
distinct kinds of filamentous fungi also were observed. In all,
the clean sediments had at least a dozen microbial forms that
were readily differentiated on the basis of morphology using a
light microscope and by examination of colonies on solid
substrates. Anaerobic microbial samples from clean reduced
sediments had mainly gram(-) bacteria (*Psuedomonas sp.*) and a
assemblage of very long (> 16 μm) gram(-) rods (probably
Desulfomonas sp., and *Desulfovibrio sp.*) which sometimes occurred
in chains. No fungi or yeast were observed to grow under
anaerobic conditions, but samples from reduced microcosms exposed
to air did show growth of a fungus. The probable identities of
the bacterial cells given above was consistent with cell
morphologies, growth conditions, and Fe and S chemistry observed
in the microcosms. With respect to sulfur, a complex system of
biogeochemical processing was indicated by analyses of extracts
and headspace from the microcosms and cultures. Under oxidized
conditions, only trace sulfides were detected leaving the gas
traps of the microcosms, and Fe and Mn species appeared as
adsorbed films and deposits on surfaces. Reduced microcosms had
strong sulfide odors, primarily H_2S, with much lower levels of
other reduced sulfur species (e.g., DMS) also evolving.
Elemental sulfur (S8) was detected in DCM extracts of the reduced
sediments, undoubtedly resulting from microbial reduction of
dissolved sulfate. When microbial isolates from the microcosms
were grown aerobically in media containing low levels of
dissolved sulfate, but high levels of DMSO as a carrier solvent
for the NOSHs, dimethylsulfone was identified in the extracts.
Under facultative anaerobic and reducing conditions in these
cultures, the microbial communities reduced the DMSO to
dimethylsulfide (DMS), which was the most prominent sulfur
species in the headspace, with relatively smaller amounts of
methane, hydrogen sulfide, and methyl mercaptan also observed.
The addition of NOSHs to these cultures caused reduction, but not
elimination of DMS production.

The diversity of the sediment microbial communities in the
stirred Eh microcosms were affected by NOSHs. Within 7 days of
the addition of the NOSH mixture to the microcosms, aerobic
samples showed reduction or elimination of gram(+) bacteria and
virtual elimination of fungi. The bacterial communities became
clearly dominated by no more than four nondescript gram(-)
species including motile and sessile rods (*Psuedomonas sp.*), two

prominent sulfur transforming species (probably *Thiobacillus sp.,*
Desulfovibrio sp.) and an actinomycete (probably *Nocardia sp.*).
Occasionally, endospore forming gram(-) rods capable of aerobic
growth (i.e., *Bacillus sp.*) also were observed in the NOSH
contaminated sediments.

Unlike the aerobic microorganisms, the anaerobic community
did not change appreciably after the addition of the NOSHs. That
is, in reduced microcosms the same general collection of cells
was observed before and after NOSH addition. NOSH enrichment
cultures and media containing NOSHs in coal carbon black as
growth substrate supported rapid growth mainly of the
psuedomonads, with the large sulfur bacteria also observed at
lower abundances. Single compound growth (e.g., on benzothiazole
and quinoline) favored mainly one or two species of psuedomonad,
with the actinomycete showing aggressive growth only when co-
substrates were introduced along with the NOSHs (e.g., alkanes,
aromatics and PAHs in petroleum or coal carbon black).

In sum, the addition of NOSHs to the microcosms reduced the
diversity of the aerobic microbial community in all the sediments
but did not appreciably affect the anaerobic community. The most
obvious changes in the aerobic microbes were: 1) drastic
reduction or elimination of viable fungi, 2) reduction of gram(+)
species, 3) emergence of a small number of dominant gram negative
rods that could metabolize NOSHs. These community alterations
undoubtedly were the result of toxicity and substrate limitation.
With respect to toxicity, elimination of fungi and reduction of
microbial numbers and diversity has been documented in sediments
contaminated with PAHs (Catallo and Gambrell 1987). The
sensitivity of fungi to promutagens such as PAHs and NOSHs (see
mutagenicity data above) can result from enzymatic processes not
found in bacteria (e.g., cytochrome P-450 systems). The removal
gram(+) bacteria and opportunistic dominance of gram(-) forms
probably corresponds to physiological differences: gram(+)
bacteria lack protective outer membrane lipid coats
characteristic of gram(-) forms (Catallo 1991). As a result,
diffusion of hydrophobic contaminants to the cytoplasm and
organelles of gram(+) bacteria is relatively rapid. A notable
exception was an actinomycete, probably *Nocardia sp.* that was
isolated from the oxidized microcosms and showed growth in the
presence of several individual NOSH compounds and simple
mixtures.

As said, the gram(-) cells that dominated in the sediments
after the addition of NOSHs were primarily *Psuedomonas sp.* with
occasional presence of *Bacillus sp.* also noted. The psuedomonads
were capable of growth on NOSH compounds such as benzothiazole
and quinoline as sole carbon sources and were characterized by
the development of dark green color in mature cultures under
anaerobic conditions. The introduction of air to these green
cultures eliminated the color immediately upon shaking. Within

43

12 hours, the green color returned as oxygen levels were decreased to low levels.

The relatively simple collection of dominant psuedomonads observed in the microcosms after NOSH addition was grown collectively in nutrient media and NOSH-amended broths on the benchtop. These were used as adapted inocula for metabolic studies on NOSH transformation pathways and preliminary biotreatment approaches (below). The metabolic specificity of this community was found to be very broad. For example, addition of these organisms to coal carbon black containing PAHs and NOSHs gave evidence of extensive degradation of different compounds within two weeks (Fig. 13). Similar work showed that a range of aliphatic and aromatic compounds in south Louisiana crude oil (SLC) were metabolized by the organisms.

NOSH Fates in the Sealed Batch Vial Microcosms

The purpose of the controlled Eh/pH microcosms (above) was to evaluate the relative effects of Eh and sediment texture on NOSH transformation with time under well controlled conditions. Clearly, the control of bulk phase redox potentials in the stirred microcosms gave rise to chemical and physical conditions not typically encountered in natural settings. Hence, data collected from the continuously stirred and bubbled systems were influenced by processes not typical of natural sediments (e.g., increased contact between sediment surfaces and the bulk aqueous phase). The unstirred, sealed batch vials of this study were used to more closely approximate conditions encountered in marine and wetland sediments. In these systems, oxidized vs. reduced conditions were maintained but not controlled within tight bounds, and conditions typical of unconsolidated sediments were achieved. Analyte losses resulting from volatilization were eliminated because the systems were sealed and not sparged with air or stirred. Chemical and physical surface effects arising from continuous mixing of particles with water also were minimized.

The results from duplicate batch vial runs on the three sediments under oxidized and reduced conditions are presented in Figures 14 - 16. For simplicity, data are presented only for those NOSH compounds showing transformation vs. killed controls. It is immediately clear from these data that: 1) the varaibility in NOSH concentration within and between time points was higher than the controlled Eh microcosms and, 2) the time course transformation of most NOSH compounds was minimal or incomplete relative to the controlled Eh microcosms. These data reflect the great variability and patchiness characteristic of environmental systems: without the influence of continual stirring and bubbling as in the controlled Eh systems, the physicochemical and biochemical properties of systems became anisotropic and heterogeneous.
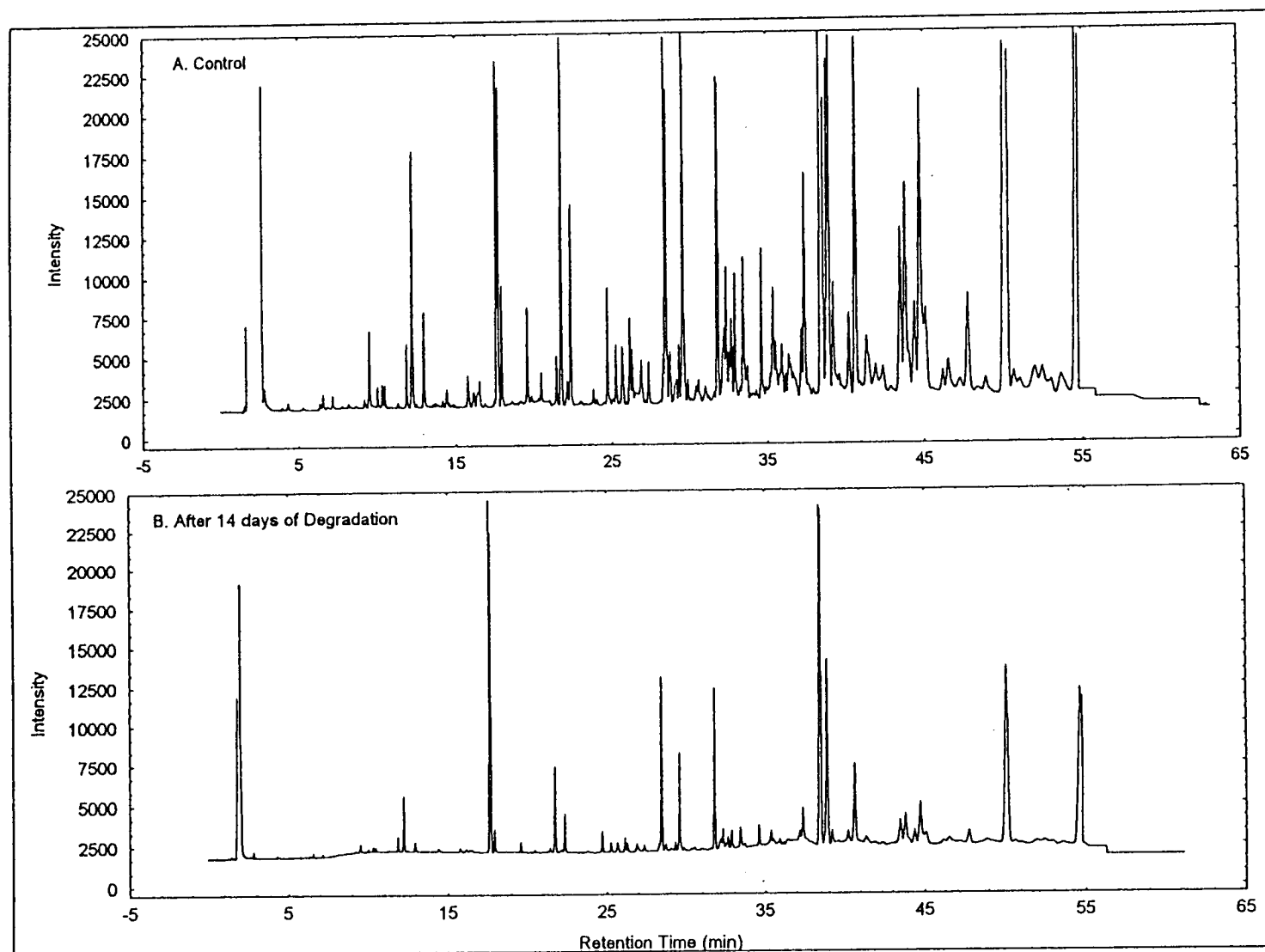
Figure 13. Biodegradation of aromatic hydrocarbons and NOSHs by microbes isolated from the controlled Eh microcosms. A. Gas chromatogram of starting mixture (aromatic fraction). B. Gas chromatogram of the mixture after 14 days of incubation with the microbes.
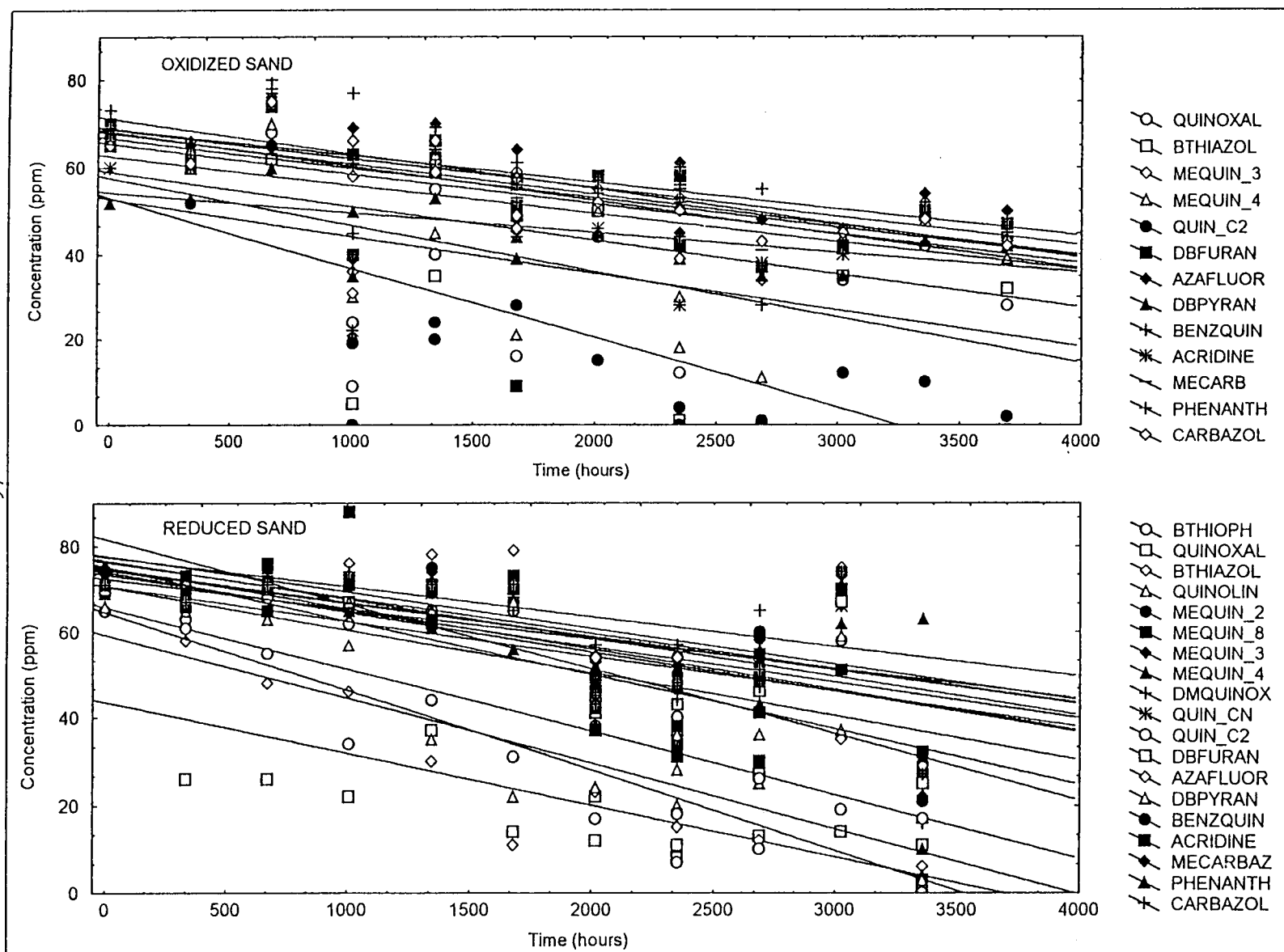
Figure 14.   NOSH transformation profiles under oxidized and reduced conditions in unstirred sand microcosms.
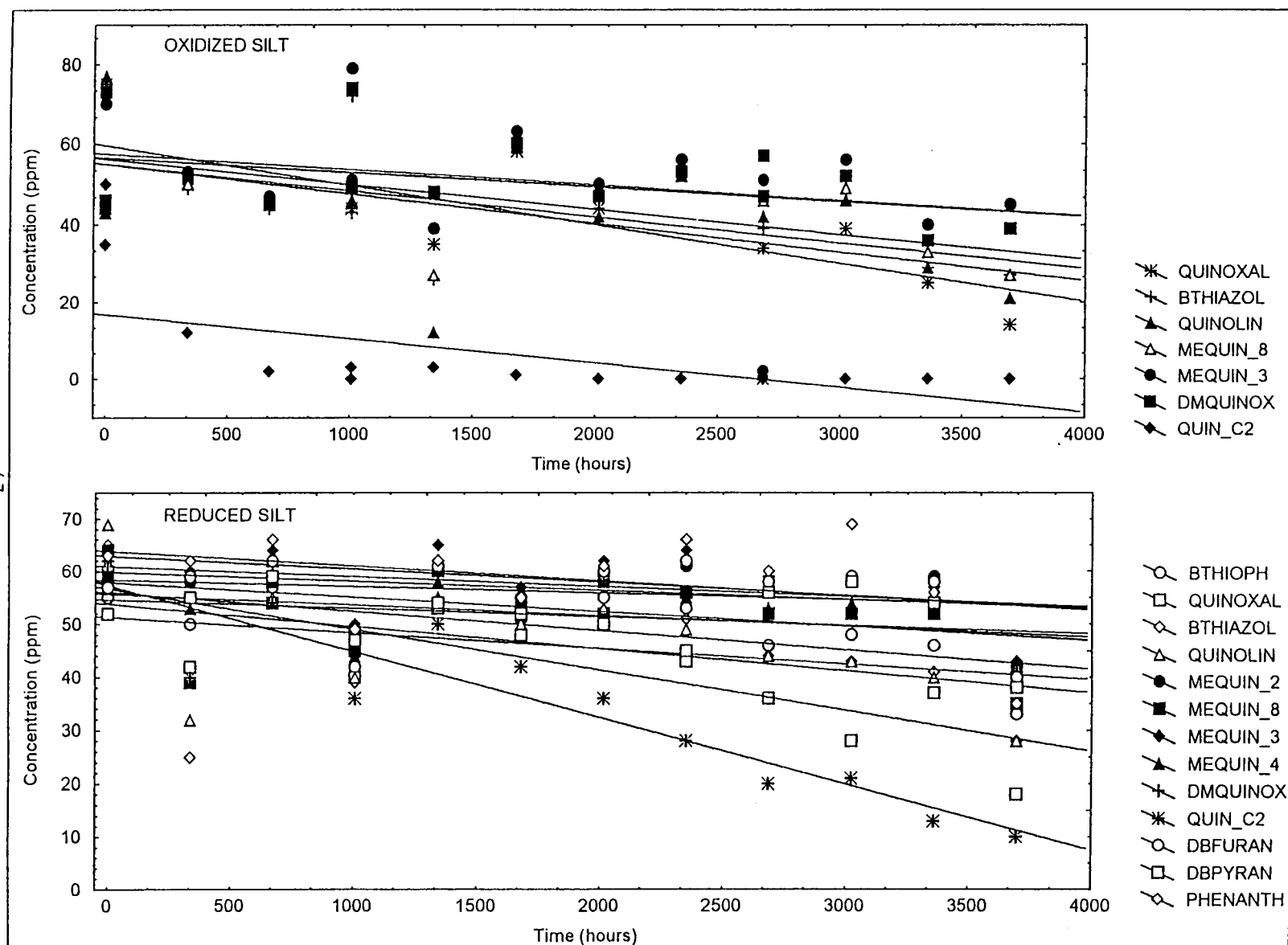
Figure 15. NOSH transformation profiles under oxidized and reduced conditions in unstirred silt microcosms.
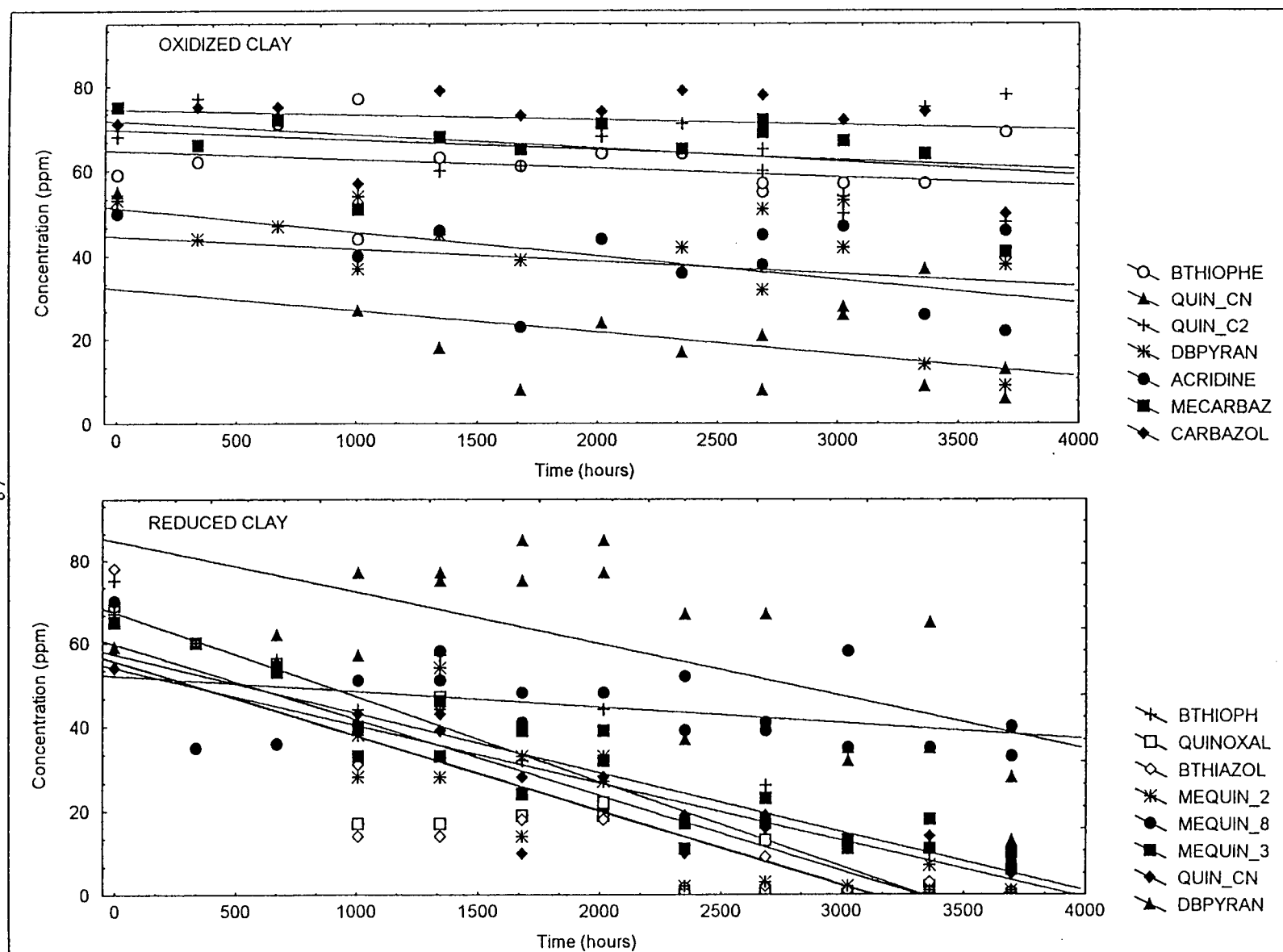
47

Figure 16. NOSH transformation profiles under oxidized and reduced conditions in unstirred clay microcosms.

Unlike the controlled Eh microcosms there was a consistent redox
effect across the three sediments in the unstirred batch vials:
significant NOSH transformation was observed for a larger number
of compounds under reduced vs. oxidized conditions within each
sediment. Also unlike the stirred microcosms, the effect of
decreasing particle size was to decrease the transformation rate
of virtually all NOSHs (i.e., the trend was not as strong in the
the stirred systems).

In oxidized and reduced sand (Fig. 14), many of the NOSH
compounds were transformed during the 3600 h incubation.
Significant linear fits of duplicate concnetration data indicated
that quinoline, quinoxaline, 4-methylquinoline, 8-
methylquinoline, quinoline carbonitrile, and 2,4-
dimethylquinoline weres most rapidly transformed. The other
NOSHs, particularly benzo(f)quinoline, acridine, phenanthridine,
dibenzopyran, and 4-azafluorene were degraded slowly, and at
roughly equal rates. Under reduced conditions, virtually all
NOSHs examined were transformed to some extent, with the highest
rates observed for benzothiazole, quinoline, 8-methylquinoline,
2,4-dimethylquinoline, and dibenzopyran.

The NOSHs were transformed to a lesser extent in the
oxidized and reduced silt than in the comparable sand microcosms.
This would appear to be a result of increased particle surface
area in silts vs. sand. While quinoxaline, benzothiazole,
quinoline, 8-methylquinoline, 3-methylquinoline, and 2,4-
dimethylquinoxaline showed minor degradation under oxidized
conditions, 2,4-dimethylquinoline was the only NOSH degraded
substantially. Under reduced conditions, 2,4-dimethylquinoline
and quinoxaline were transformed most rapidly, with other NOSHs
(e.g., benzothiophene, benzothiazole, quinoline, and 8-
methylquinoline) showing slower rates.

In oxidized clay, only benzothiophene, quinoline
carbonitrile, 2,4-dimethylquinoline, dibenzopyran, acridine, 9-
methylcarbazole, and carbazole showed evidence of very minor
degradation. Under reduced conditions, however, 2,3-
benzothiophene, quinoxaline, 2-methylquinoline, 3-methyl-
quinoline, 8-methylquinoline, quinoline carbonitrile, and
dibenzopyran showed significant amounts of degradation, with
significant amounts of transformation products accumulating in
the extracts.

The stirred and unstirred microcosm data suggested that, 1)
NOSH compounds are transformed slowly under quiescent conditions
found widely in field settings, 2) data from stirred microcosms
provided little predicative information on NOSH behavior in
sediments maintained under more realistic conditions, 3) NOSH
transformation rates from chemical and microbial processes
decrease as particle size decreases from sands to clays, 4)
stirring of sediment-water containing can increase NOSH
degradation rates relative to undisturbed sediments of the same
particle size and redox conditions, 5) under quiescent

conditions, NOSHs tend to be more labile in reduced than oxidized
sediments, but stirring attenuates this effect and, 5) the
removal of stirring as an input parameter decreased the
partitioning of NOSHs into the aqueous phase and thus slowed
their transformation rate.

The increased NOSH degradation observed in the reduced batch
vial microcosms suggested that complexation reactions with redox
active metals was an important factor in NOSH degradation. There
was evidence that most chemical and biochemical transformation of
NOSHs occurred in the aqueous phase rather than at surfaces, and
desortpion of precipitated NOSH-metal complexes under reducing
conditions could account for the redox effect on degradation. In
order to examine this, mixtures of NOSHs were dissolved in DCM
and shaken in seperatory funnels with deionized water or
deionized water containing ferric ($FeCl_3$ or $Fe(OH)_3$) or ferrous
iron ($FeSO_4$). The oxidized and reduced forms of iron (solid
$Fe(III)$ and soluble $Fe(II)$, respectively) are found widely in
marine sediments at significant concentrations (e.g., > 50 ppm)
and have been shown to complex some azaarenes (Jorgensen et al.,
1985; Stetter et al., 1985). After extended shaking, the phases
were seperated and the DCM was dried and analyzed using GC (Fig.
17). The data from these partitioning experiments indicated that
both dissolved and particulate forms of iron could facilitate
removal of the NOSHs from the DCM organic phase into the aqueous
phase. Thus, the pure water controls (Fig. 17) show retention of
the NOSH compounds in the DCM after shaking, while the presence
of iron increased the tendency of some NOSHs to partition with
the water. The effect was much more pronounced with ferric than
ferrous iron. This showed that insoluble $Fe(III)$ as found under
oxidized conditions in sediments was capable of complexing many
NOSHs thereby changing their phase partitioning behavior during
extractions with DCM, and decreasing recoveries. Hence, oxidized
sediment slurries containing appreciable amounts of labile iron
could develop an insoluble phase that allows for significant
complexation reactions to occur. Under reduced conditions,
reduction of $Fe(III)$ to soluble $Fe(II)$ and subsequent dissolution
of colloids would allow for liberation of NOSHs to the aqueous
phase where they would be available to chemical and biochemical
reactions. While still complexing some NOSHs (quinoline, 2-
methylquinoline, 4-methylquinoline, quinoline carbonitrile) and
limiting their partitioning with DCM, the effects soluble $Fe(II)$
on the recovery of most compounds was insignificant.

Molecular modelling was performed on a variety of postulated
NOSH-Fe(III) complexes. A minimum energy configuration for one
possible complex between quinoline and $Fe(OH)_3$ was provided by
MMX force field approaches:

D: 2.510	D: 2.347
QQ: -0.339	QQ: -7.217
VDW: 6.261	VDW: 3.052
Tor: 14.223	Tor: 14.244
Hf: 44.10	Hf: -38.76
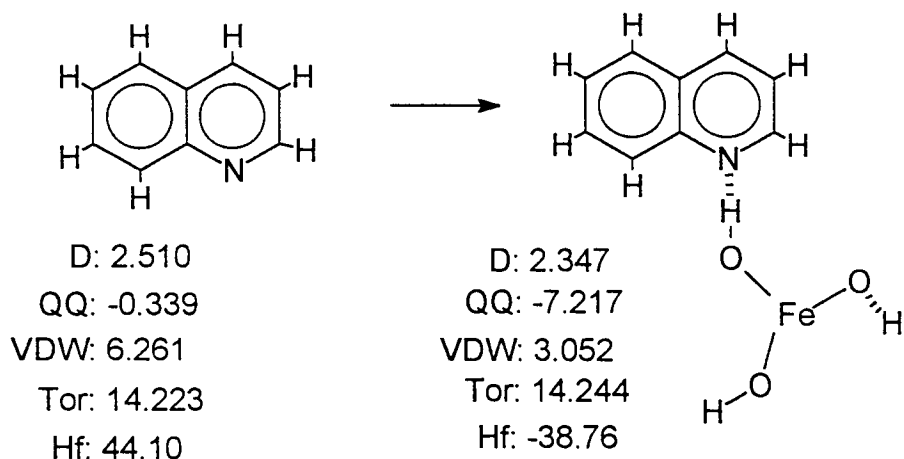
where the radius of Fe is taken as 1.26 A, D is dipole moment in debyes, Hf is heat of formation (kcal/mole), and Tor, QQ, and VDW are components of total energy from torsion, charge-charge repulsions and Van der Waals forces, respectively (all kcal/mole). Although D and Tor values were not significantly altered by formation of the proposed complex, VDW and QQ values were significantly decreased in the complex vs. the free base. This suggested that the electrostatic interaction (H-bond) between the quinoline nitrogen and the iron hydroxide proton attenuated attractive intramolecular forces (VDW) between the nitrogen and vicinal protons on the quinoline rings. QQ repulsions also were decreased in the proposed complex, possibly by alteration of the normal zwitterionic character of pyridine-based heterocycles (Catallo et al., 1990a). Most significant however, was the negative Hf for the complex. This indicated that this reaction is thermodynamically favorable and thus supports interpetations regarding the importance of metal complexation on liquid phase distributions given above. (It is not possible to model ionic species with the MMX algorithms. One would expect direct electrostatic interactions between the heterocyclic free base and the metal atom; q.v., Stetter et al. 1985). The same calculations were performed on the other NOSHs with similar results. In general, these calculations suggested that the N and, to a lesser extent, S- and O- heterocyclic compounds were able to form stable metal complexes with Fe species. The data in Fig. 17 and the modelling example with quinoline shown above provides a mechanism by which chemical conditions in oxidized sediments could adversely affect the degradation and solvent extraction recoveries of NOSH compounds. The target NOSHs in the microcosms had extended equilibration times (24 - 2500 hours) and ample opportunity to contact active surfaces and adsorbed reactants. Although not studied explicitly, it is likely that equilibration times on the order of hours was sufficient to affect the chemistry and recovery of the
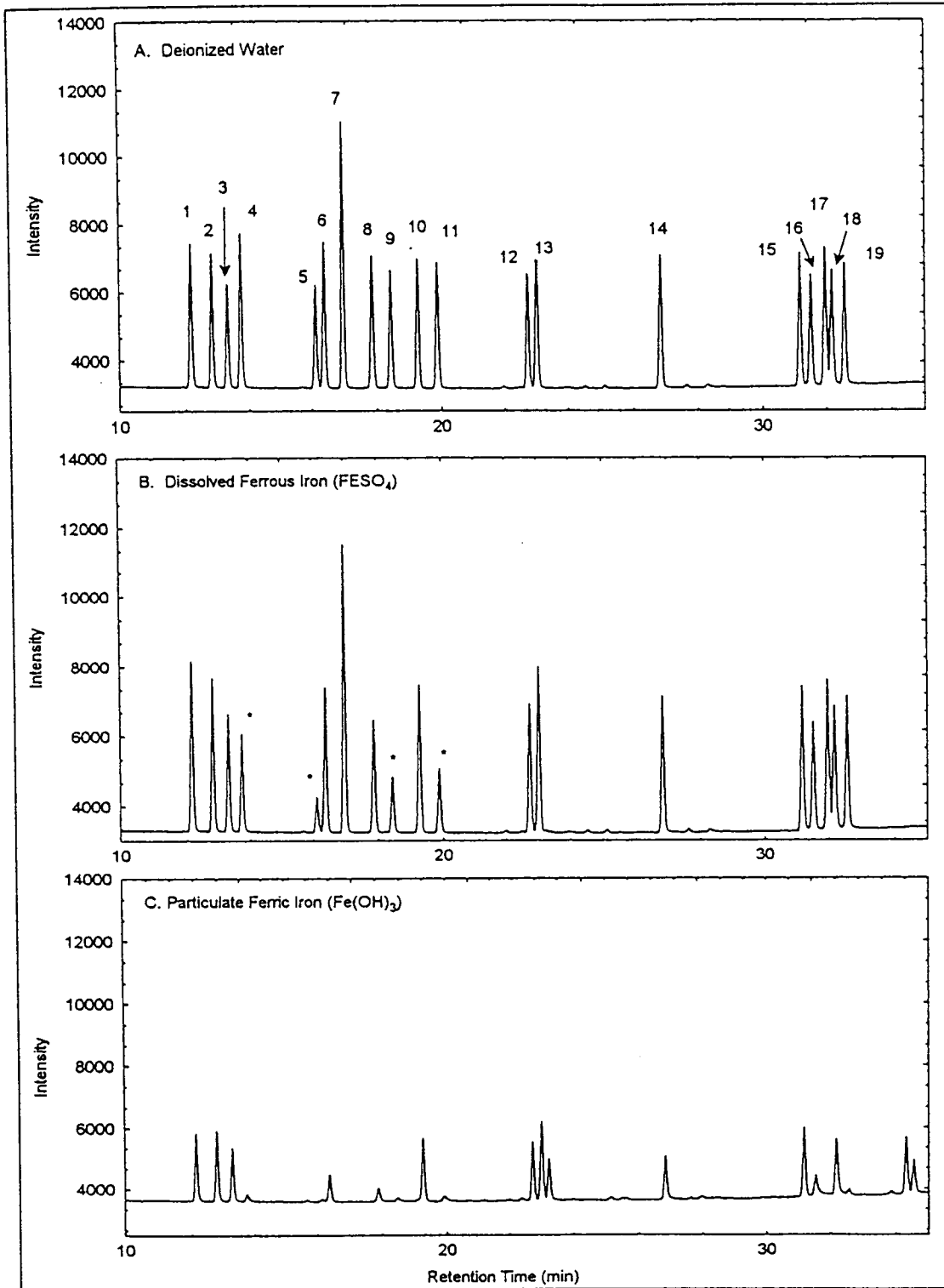
Figure 17. Extraction of NOSHs from organic solvents into water: effects of Fe(II) and Fe(III) complexation on NOSH compound recovery from DCM. Peak numbers correspond to compounds identified in Figure 4.

52

NOSH compounds, as was clearly indicated for some of the indole and pyran based NOSHs in the microcosms and in the partitioning experiments summarized in Fig. 17. Further work on adsorption-desorption, metal complexation/catalysis, and redox effects on NOSH compounds would be interesting and productive for understanding NOSH fates in environmental systems.

The effect of metal complexation on NOSH compound recovery could have been surmounted by a number of treatments, probably the most straightforward being acidification of the sediments during extraction, followed by adjustment of pH in the final extract. This was not done because of 1) the desire to avoid inevitable analyte losses that accompany these treatments and, 2) the need to avoid reaction/degradation of NOSH transformation products also found in the microcosm extracts. The tendency of oxidized sediments to sequester NOSHs as insoluble metal complexes suggested a possible remediation approach for these materials in sediments. In cases where NOSHs are found as significant elements of waste mixtures (e.g., creosote, coal tars, asphalts, ash), establishment of reducing conditions via flooding and addition of organic carbon followed by passive leaching could be effective in removing NOSHs from adsorption sites on sediments and oxidized Fe colloids. Preliminary experiments done in this laboratory have shown that some NOSHs are very mobile in sediments under these conditions, primarily as soluble metal complexes and protonated salts, as shown below.

hydrophobic
free base

H^+
pH 4.5

hydrophilic
ion pair

X^-
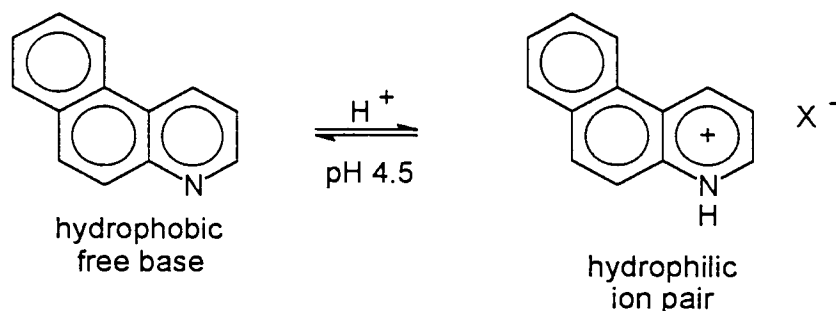
Remediation approaches using acids (soil washing, electro-kinetics) also could remove some NOSHs from contaminated sediments and slurries, thereby simplifying the matrix for further treatment. The toxicological implications of matrix simplification in this way, however, need to be examined.. Clearly it would be undesirable to decrease chemical complexity of mixtures if this results in increased toxicity (q.v. Table 3).

Metabolic and Deuterated Tracer Studies in Liquid Cultures

In order to further characterize the biodegradation of NOSHs by the bacterial community discussed above, metabolic pathway studies were conducted on representative compounds vs. killed controls. It was found that quinoline and other light azaarenes were metabolized with little or no accumulation of stable

intermediates, but results from stable isotope studies will be needed before this can be stated with confidence. Other compounds, such as benzothiazole and benzo(f)quinoline also were transformed, but a wide range of stable intermediates were accumulated in the culture media.

In order to examine transformation pathways and certify the identity of postulated transformation products, benzo(f)quinoline and benzothiazole were synthesized in deuterated form for use as stable-isotope tracers. Mass spectra for the protiated and deuterated homologs for each compound are shown in Fig. 18 and 19. The difference in the isotopic structures of the protiated and deuterated homologs can be easily seen in these figures. The tracer compounds were added to minimal media conatining the bacterial community and incubated for various periods, followed by extraction and analysis of products using GC-MS.

With respect to benzo(f)quinoline, the major stable metabolite observed using the protiated compound had a molecular ion at m/z 195 (Fig. 20 A). This molecular ion, and logical losses corresponding to oxygen suggested that the identity of the metabolite was 5(H)-6-benzo(f)quinoline-one, although the corresponding phenol also would be consistent (as shown below). Parallel runs using the deuterated benzo(f)quinoline homolog also produced a major product with a single oxygen atom, which at first glance seemed to confirm the identification derived from
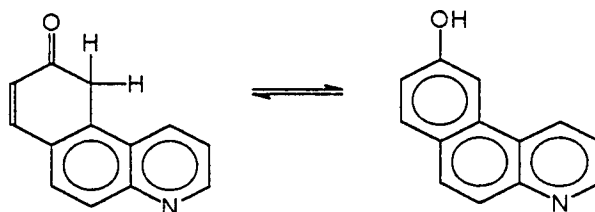
Benzo(f)quinoline oxidation products consistent
with the mass spectrum shown in Fig. 20 A (m/z 195).

the protiated run (i.e., the phenol or quinone shown above, Fig. 20B). But, if one accurately calculates the masses involved it becomes clear that a ketone or phenol derivative of the deuterated compound would have a molecular ion of m/z 203, which was not found associated with any peaks in the extracts from the deuterated tracer runs. The only structure with mass 204 that would be consistent between the protiated and deuterated experiments is a benzo(f)quinoline epoxide, probably the 9,10 epoxide (shown in Fig. 20B). In the protiated system Fig. 20A), this epoxide would have the appropriate mass (i.e., 195). Hence, a major benefit of the deuterated tracer approach is illustrated by this example: in cases where multiple structural assignments are possible from mass spectral data of unknown compounds, parallel protiated-deuterated tracer data can be used to
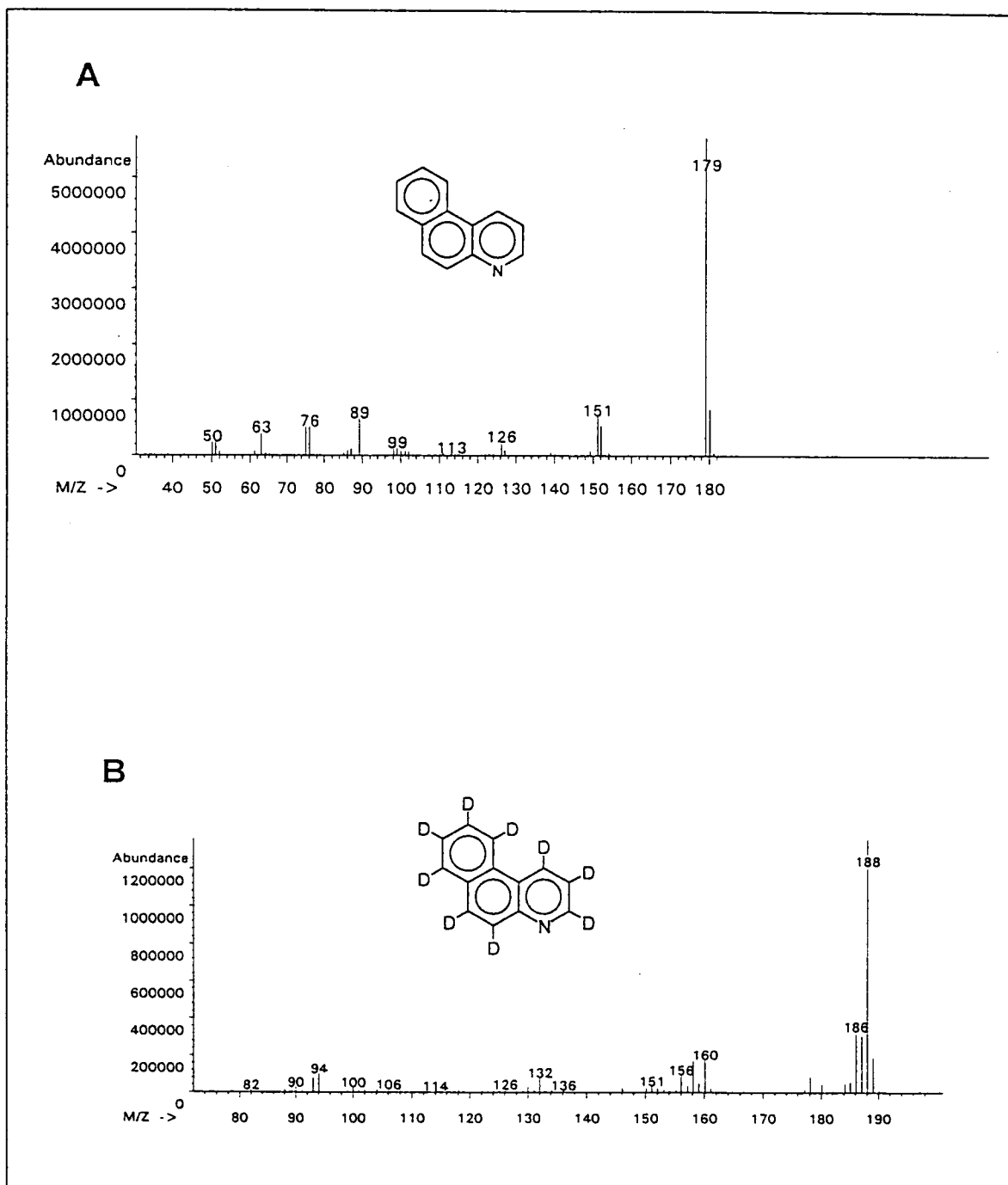
Figure 18. A. Mass spectrum of benzo(f)quinoline. B. Mass spectrum synthetic benzo(f)quinoline-d9.
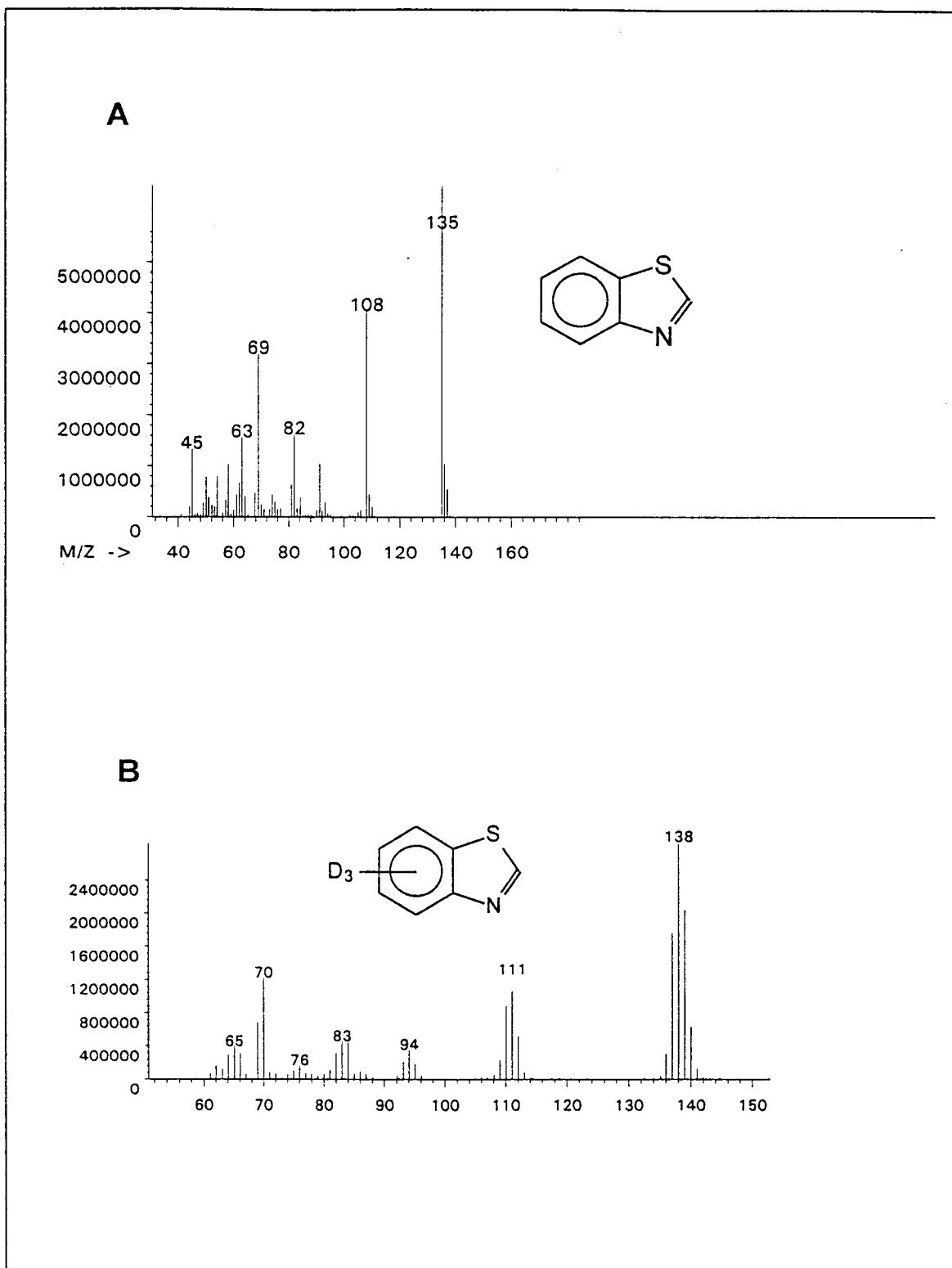
55

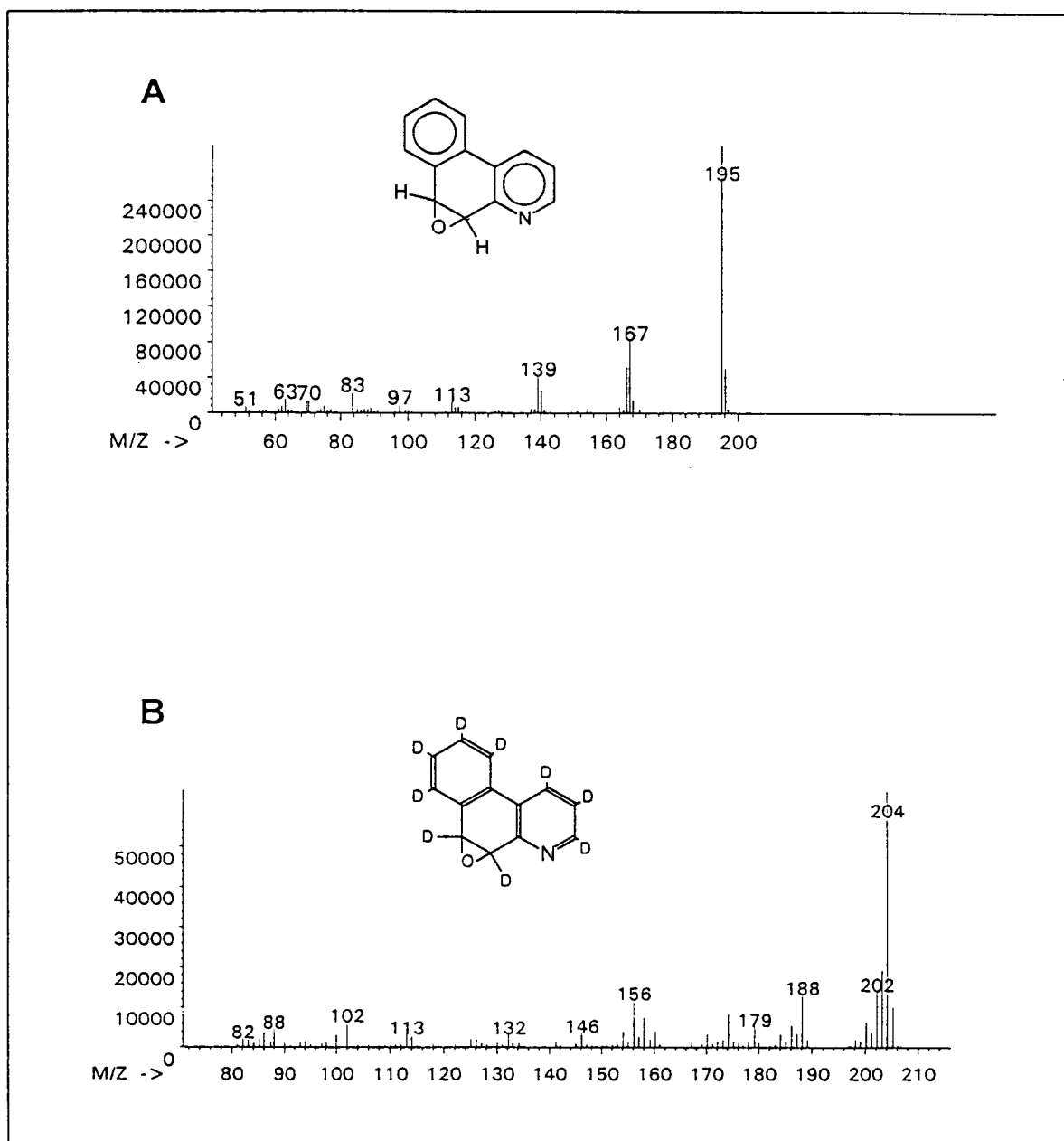Figure 19. A. Mass spectrum of benzothiazole. B. Mass spectrum of synthetic benzothiazole-d3.

Figure 20. A. Mass spectrum of a benzo(f)quinoline transformation product. B. Mass spectrum of the same product from the deuterated tracer experiments. (Only one possible isomer is shown.)

determine the identity of the compound in question. In the
present instance, this ability had profound significance. The
unequivocal presence of the benzo(f)quinoline epoxide as a major
metabolic product in these experiments was striking for two
reasons: 1) these epoxides are almost certainly the result of
eukaryotic enzyme systems, but the microbiological data
summarized above indicated that fungi had been severely impacted
by the NOSHs. It would seem that either the microbiological data
were erroneous (i.e., there were significant levels of viable
fungi in the microcosms after addition of the NOSHs), or some
other eukaryote (e.g., protozoan, algae) that was not observed
was responsible for major metabolic transformation of this
material. 2) Epoxides of many polycyclic aromatic systems are
proximal mutagens, and the benzo(f)quinoline species identified
in the extracts is very similar in structure to known mutagens
and teratogens (Lehr and Jerina 1983; Ho et al. 1984). The
molecular modelling and toxicity work of Lehr and Jerina (1983)
showed that the position of the heteratom vis a vis the epoxide
moiety was important in determining the degree of mutagenicity of
the heterocycle. Data generated in this work showed that
phenathridine also was transformed to an epoxide, and data on the
relative toxicity and mutagenicity of this species vs. the other
benzoquinoline isomers (acridine, benzo(f)quinoline,
benzo(h)quinoline, etc.) would be very interesting and is
important to evaluating the toxicological significance of these
materials in environmental waste mixtures.

      These data also strongly suggest that formation of epoxides
by marine microbes seems likely for higher NOSH ring systems such
as the benzacridines, azafluroanthenes, and azabenzopyrenes, all
of which can occur in crude oils, coal chemicals, and pyrogenic
mixtures (Adams et al. 1982; Beiko et al. 1987; Zitko 1980; Turov
et al. 1987; Wakeham 1979; Furlong and Carpenter 1982) and many
of which are potent carcinogens (Lehr and Jerina 1983).

      The results of the benzothiazole tracer studies were even
more compelling than the benzo(f)quinoline work shown above. The
mass spectra of protiated and deuterated benzothiazole are given
in Fig. 19, and the difference in isotopic structures of the
molecular ions and fragments between the two homologs is obvious.
Many of the metabolic transformation products found in the
microcosms and media experiments using protiated benzothiazole
(Fig. 10) also were observed in the deuterated tracer
experiments. In general, a wide range of addition products
including alkylated and glycolated benzothiazoles were found
along with oxidized species, and a suite of products with
molecular weights much above the starting material (Fig. 21).
This spectrum of transformation products was very similar to
those seen in biochemical reactions of thiamine, which has a
thiazole ring active site. Reactions involving carbanion
intermediates, and subsequent glucoaldehyde formations with
thiamine (e.g., in transketolase enzymes, below) are essential to

pentose phosphate cycle (Fersht, 1985). As shown below, intermediates these reactions in vivo can include reduced

Thiamine (Vitamin B1)
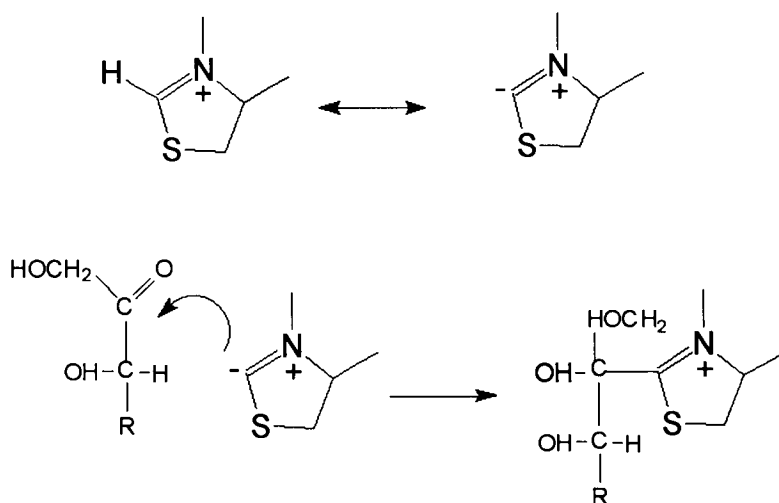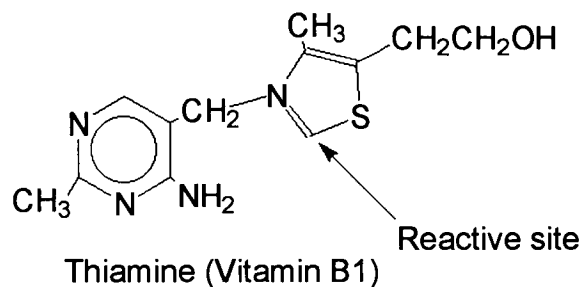
Typical addition reactions of thiazole active
sites in the thiamine coenzyme

thiazole and its alkyl substituted homlogs including glucoaldehydes and thiols. The products of benzothiazole and its deuterated homolog were precisely of these types (Fig. 21, 22), and this strongly suggested that benzothiazole competed with thiamine for transketolase enzyme active sites. This phenomenon could account for toxicity of benzothiazole (i.e., as a biomimetic toxicant) and its disappearance from the microcosms (i.e., it was assimilated and transformed as well as degraded). A range of other deuterated compounds were observed in the tracer runs of benzothiazole, but these have not submitted to identification (Fig. 23). Further, there was evidence of biochemical oxidation reactions which gave rise to exotic addition products including anilobenzothiazole and dimeric bis-2,2'-benzothiazole. These products indicated that $1H^+/1e^-$

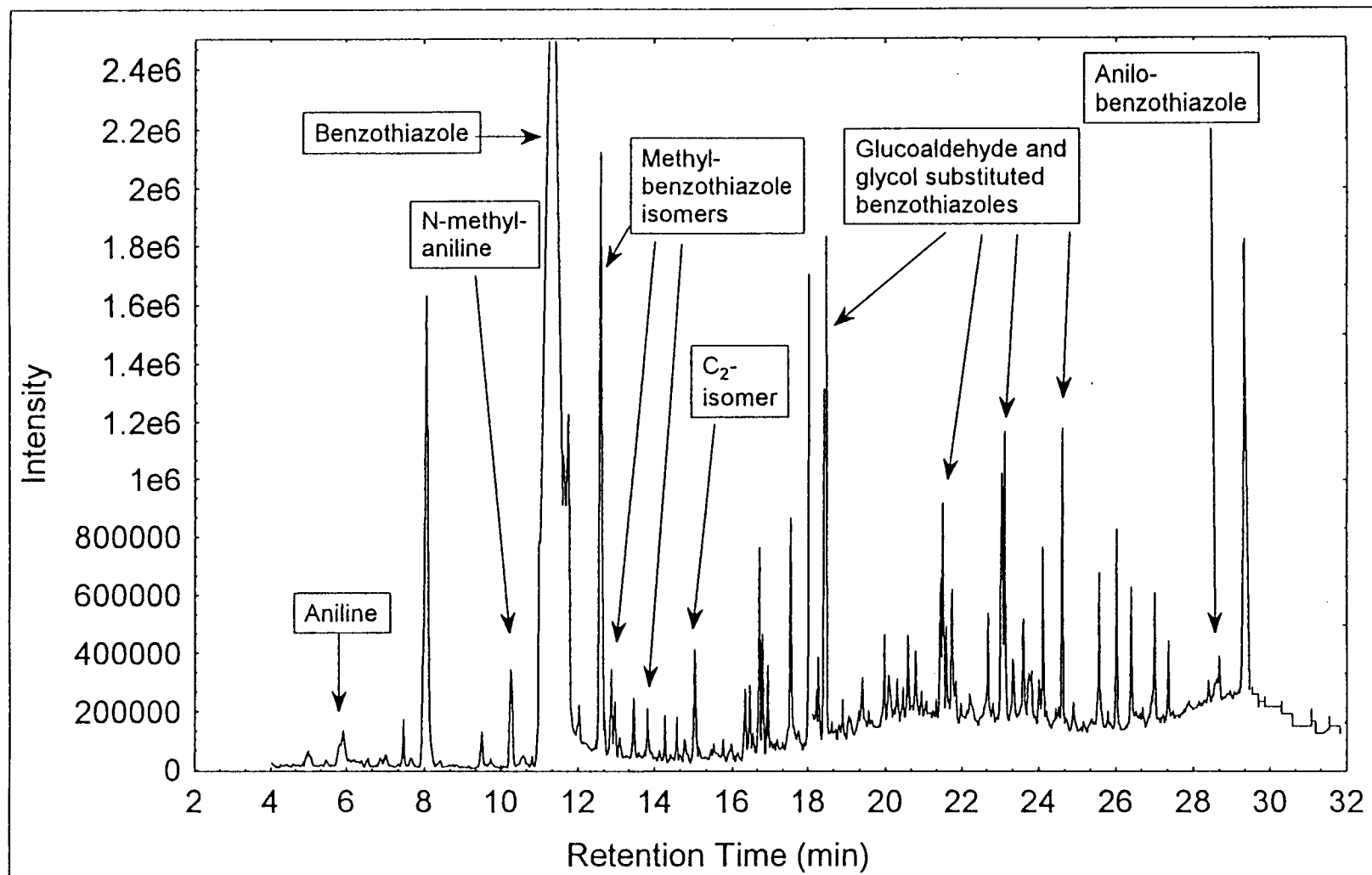Figure 21. Total ion chromatogram of benzothiazole tracer experiment showing the starting material and transformation products in the extract.
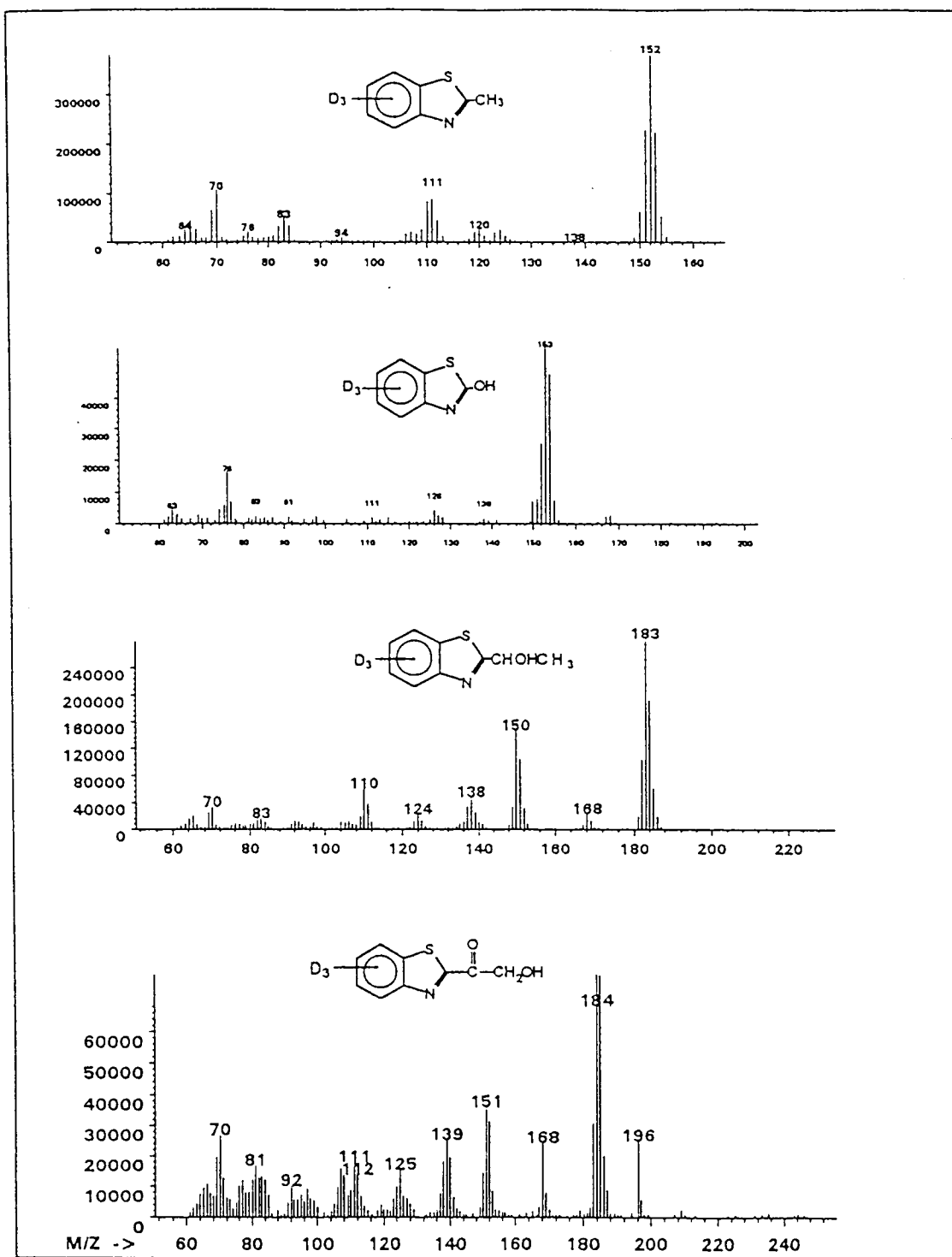
Figure 22. Mass spectra of benzothiazole transformation products
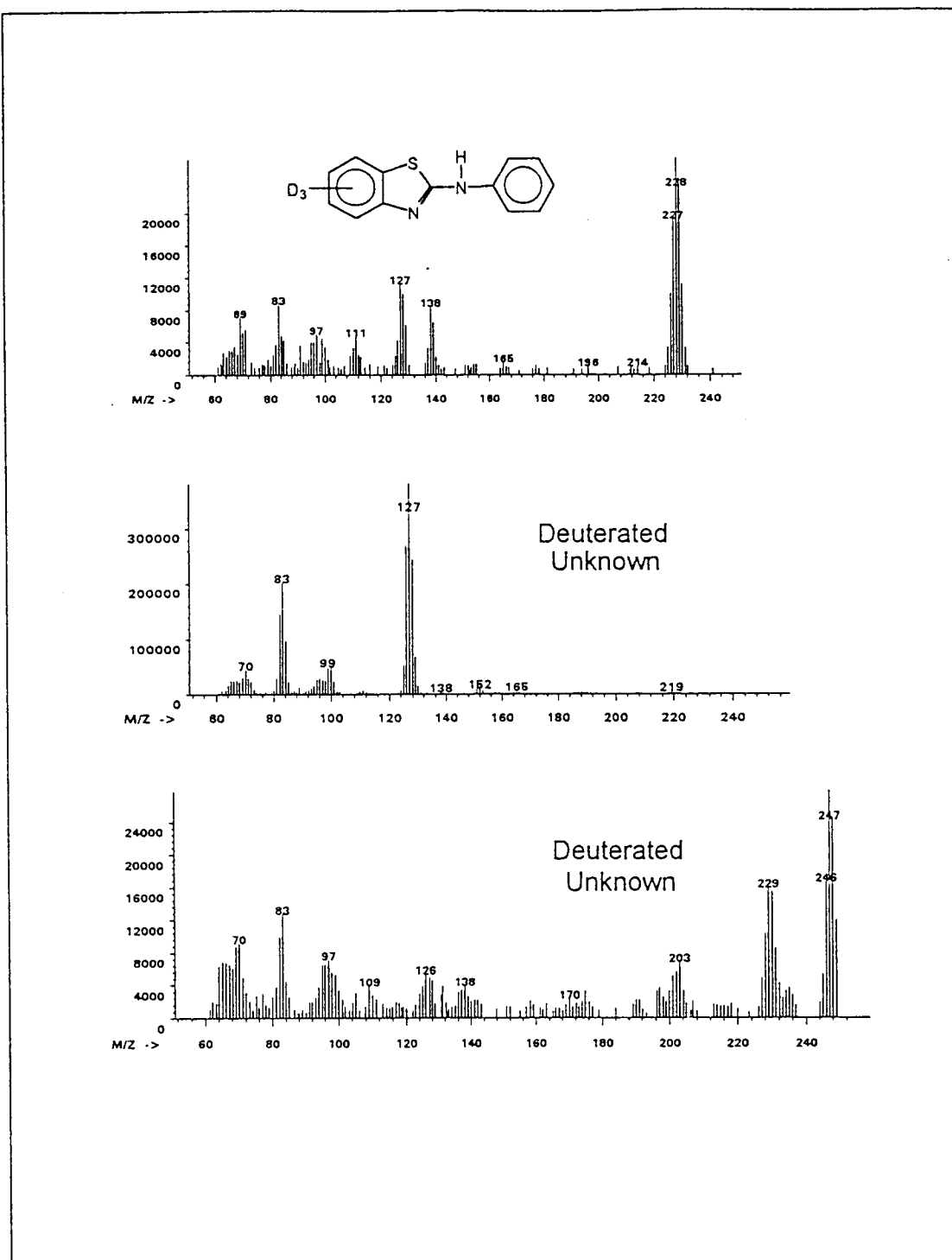identified in protiated and deuterated pathway experiments.

Figure 23. Mass spectra of benzothiazole transformation products and unknowns found in the protiated and deuterated pathway experiments.

62

oxidations of benzothiazole at the acidic 2-proton were followed by recombination to the dimer or reaction with other amines including aniline. This mechanism was confirmed by the results of electron transport studies between benzothiazole and iodonitrotetrazolium violet (Catallo et al. 1990b) followed by product analysis using magnetic sector mass spectrometry with "soft" ionization (i.e., fast atom bombardment). Although the presence of anilobenzthiazole in these systems was virtually certain (it was identified in protiated and deuterated runs), the origin of the aniline in the system was unclear: the aniline apparently was not a synthetic contaminant or primarily a degradation product of the benzothiazole. Much further work on this fascinating system is called for in light of data presented here. It is possible that the chemical and biochemical reactions observed in this work could form the basis of biotechnological generation of specific benzothiazole metabolic products for use in organic synthesis, pharmacological research (Bohacek and McMartin 1994), drug design, or specific molecular probes.

CONCLUSIONS

Relative to estuarine water and microbial cultures NOSH compounds are degraded slowly and incompletely in sediments under conditions found in many estuarine, wetland, and marine settings. Turbulent mixing in high energy areas may increase the availability of NOSHs to relatively rapid chemical and microbiological reactions in the aqueous phase, but these conditions pertain only a small proportion of the total volume of wetland and coastal systems likely to receive NOSHs from energy and urban/industrial activities.

Under continuously stirred conditions, compounds such as quinoline and its alkyl homologs and will degrade to prosaic products under oxidized and reduced conditions. Other NOSHs such as acridine, benzo(f)quinoline, and benzothiazole apparently are transformed to stable products, some of which have high toxicity and mobility. In stirred sediment-water slurries, NOSH degradation processes are decreased by increased particle surface area and reduced electrochemical conditions. That is, degradation is fastest in oxidized sediments of large particle size when physical mixing of the system is vigorous. In unmixed, standing sediments, NOSH degradation rates also are decreased by increasing particle surface area (i.e., decreasing particle size), but are promoted by reducing electrochemical conditions. This supported the idea that most biochemical and chemical transformations of significance to NOSH fates in situ occur in the aqueous phases of the sediments and slurries, rather than at surface sites on particles. In cases where particle surface area is high, sequestration of NOSHs can occur and increase their persistence, even in well mixed sediment-water systems. Processes that liberate NOSHs from sediment surfaces to the aqueous phase (protonation, complexation) can be expected to increase the degradation of some NOSHs relative to rates on sediment surfaces, but this also can give rise to increases in aqueous phase toxicity.

There is empirical and theoretical evidence to suggest that complexation of redox-active metals played a large role in the sorption-desorption chemistry, and degradation pathways of NOSHs observed in the micocosms of this study. The unstirred microcosms showed a clear redox effect that supported this hypothesis: reducing conditions typically favored more rapid degradation of a larger number of NOSHs than oxidized conditions within a sediment type. These data suggested that the effects of stirring sediments in water (increased contact between particle surfaces and water, enhanced chemical diffusion) could remove or alter redox effects. That is, the physicochemical effects of stirring were larger than effect of electrochemical conditions with respect to NOSH degradation. As mentioned, the stirred microcosms behaved more like aqueous systems than sediments, and

this was in agreement by NOSH degradation rate data determined in estuarine water by other workers.

The toxicity data from the stirred microcosms showed general detoxification of the aqueous phases with time. It seemed likely from the time-course data that this detoxification was a multi-step process involving intermediates, which sometimes were as (or more) toxic as the starting materials. Many of the NOSH compounds formed stable, polar degradation intermediates that clearly were involved in increases in aqueous toxicity. The pathways of NOSH transformation were highly diverse, and included oxidation of aromatic rings to epoxides, phenols or ketones followed by ring opening and β oxidation of resultant hydrocarbon chains. Alkyl groups (e.g., the dimethyl quinolines) were oxidized to carboxylic acids followed by decarboxylation. Benzothiazole demonstrated a series of addition reactions along with degradative oxidation reactions. Surprisingly, the NOSH transformation product spectrum was very similar between oxidized and reduced conditions (q.v. Godsy et al., 1993). Chemical reactions including protonation, electrochemical oxidation or reduction followed by transformation, and perhaps catalytic deprotonation of relatively acidic protons also were indicated with several NOSHs.

Estuarine sediments contaminated with NOSH compounds can be expected to remain toxic for long periods, and various NOSH chemicals may leach through compositionally heterogeneous phases as metal complexes or protonated ion pairs. Possible remediation strategies include passive leaching under reduced conditions followed by microbial augmentation in stirred, aerobic bioreactors. Further research on the environmental chemistry on NOSHs is called for, particularly with respect to sorption-desorption chemistry, electrochemical reactions and hydrolysis, metal complexation chemistry, and affiliated changes in bioavailability, transformation rates/pathways, and toxicity. The deuterated tracer approaches provided by this work should provide a good base for these studies to proceed. The first author currently is evaluating the use of double labelling techniques for the purpose of monitoring trophic transfer and mechanistic toxicology of NOSHs, and as in situ tracers in field studies of biodegradation of NOSHs in waste mixtures and pyrogenic products.

BIBLIOGRAPHY

Adams, J., E. L. Atlas, and C. S. Giam. 1982. Ultratrace determination of vapor-phase nitrogen heterocyclic bases in ambient air. Environ. Sci. Technol. 54:1515-18.

Atkins, P. W. 1984. Molecular Quantum Mechanics. Oxford University Press, London, U.K., 465 pp.

Austin A. C., L. D. Claxton, and J. Lewtas. 1985. Mutagenicity of the fractionated organic emissions from deisel, cigarette smoke condensate, coke oven, and roofing tar in the Ames assay. Environ. Mutagenesis 7:471-487.

Beiko, O. A., N. N. Gerasimova, and T. A. Sagachenko. 1987. Nitrogen bases of industrial west Siberian crude oil, Petrol. Chem. USSR 27(3):200-210.

Black, J. N. P., R. M. Kauffman, D. Denney, and D. Grbic-Galic. 1993. Biotransformation of indole and quinoline under denitrifying conditions. In: Symposium on Bioremediation of Hazardous Wastes: Research, Development, and Field Evaluations. USEPA Office of Researchg and Development, EPA/600/R-93/054, pp. 232-233.

Blumer, M. (1975). Organic compounds in nature: Limits of our knowledge, Angewandte Chemie, 14(8):507-514.

Bohacek, R. S. and C. McMartin. 1994. Multiple highly diverse structures complementary to enzyme binding sites: results of extensive application of a de novo design method incorporating combinatorial growth. J. Amer. Chem. Soc. 116:5560-5571.

Burkert, U. and N. L. Allinger. 1982. Molecular Mechanics. ACS Monograph Series # 177. American Chemical Society, Washington DC, 339 pp.

Cairns, J. 1980. Estimating hazard. BioScience 30(2):101-107.

Catallo, W. J. and R. P. Gambrell. 1987. The effects of high levels of polycyclic aromatic hydrocarbons on sediment physicochemical properties and benthic organisms in a polluted stream. Chemosphere, 16(5):1053-1063.

Catallo, W. J. 1989. Effects of selected nitrogen-containing aromatic compounds (NCACs) on physiological properties in

Escherichia coli. Ph.D. Thesis. College of William and Mary, Williamsburg VA, 170 pp.

Catallo, W. J., D. R. Cleland, and M. E. Bender. 1990a. Toxicity of nitrogen-containing aromatic compounds (NCACs). Quinoline and 4-azafluorene behavior in an *Escherichia coli* test system: evidence of membrane effects. In: Landis, W. G. and W. H. van der Schalie (eds.), Aquatic Toxicology and Risk Assessment. ASTM Special Technical Publication 1096, American Society for Testing and Materials, Philadelphia, PA, pp. 199-221.

Catallo, W. J., R. J. Gale, R. L. Wong, and M. E. Bender. 1990b. The reducible dye 2-(*p*-iodophenyl)-3-(*p*-nitrophenyl)-5-phenyl-2H-tetrazolium chloride (INT) for use in aquatic toxicology. Notes on chemical structure, electrochemistry, and toxicity, In: Landis, W. G. and W. H. van der Schalie (eds.), Aquatic Toxicology and Risk Assessment. ASTM Special Technical Publication 1096, American Society for Testing and Materials, Philadelphia, PA, pp. 222 - 236.

Catallo, W. J. 1991. Use of indigenous and adapted microbial assemblages in the removal of organic chemicals from soils and sediments, Water Science and Technology, 25(3):229-237;

Catallo, W. J., R. J. Gale, and R. J. Portier. 1992a. Toxicity of quinoline and benzo(*f*)quinoline in a bacterial cell system. Environmental Toxicology and Water Quality, 7(1):1-17.

Catallo, W. J., J. B. Feix, and R. J. Gale. 1992b. Movement of methylphenazyl free radicals in polar and nonpolar liquids. Free Radicals in Biology and Medicine (Pergamon), **13**:35-40.

Catallo, W. J., D. H. Hoover, and D. Vargas. 1994. Effects of an environmental toxicant on ultrastructure in Paramecium caudatum and the protective effect of dissolved calcium. Aquatic Toxicol. 29:291-303

Cavalieri, E. L. and E. G. Rogan. 1984. One electron and two electron oxidation in aromatic hydrocarbon carcinogenesis. In: Free Radicals in Biology Volume IV, Academic Press, NY, pp. 323-369.

Chou, T. W. and N. Bohonos. 1979. Diauxic and cometabolic phenomena in biodegradation evaluations. In: Microbial Degradation of Pollutants in Marine Environments, EPA-600/9-79-012, pp. 76-88.

Collins, C. H., P. M. Lynn, and J. M. Grange. 1989. Microbiological Methods (6th Edition), Butterworth and Co., London, 409 pp.

Davis, J. C. 1986. Statistics and Data Analysis in Geology (2nd Edition) John Wiley and Sons, NY, 646 pp.

Dewar, M. J. S. and C. Doubleday. 1978. A MINDO/3 study of the Norrish Type II reaction of Butanal. J. Amer. Chem. Soc. 100(16):4935-4941.

Dewar, M. J. S. 1983. Development and status of MINDO/3 and MINDO, J. Molec. Structure, 100:41-50.

Dewar, M. J. S., E. G. Zoebisch, E. F. Healy, and J. J. P. Stewart. 1985. AM1: A new general purpose quantum mechanical molecular model, J. Amer. Chem. Soc. 107:3902-3909.

EPRI (Electric Power Research Institute). 1985. Inventory of organic emissions from fossil fuel combustion for power generation, EPRI EA-1394-TPS 78-820, 44 pp.

Fersht, A. 1985. Enzyme structure and mechanism (2nd Edition), W. H. Freeman and Co., 475 pp.

Frolov, Y. B. and N. A. Vanyukova. 1988. Alkylcarbazoles of Samotlor crude oil. Petrol. Chem. USSR, 28(3):177-83.

Furlong, E. T. and R Carpenter. 1982. Azaarenes in Puget Sound sediments. Geochim. Cosmochim. Acta 46:1385-1396.

Haugen, D. A., M. J. Peak, and K. M. Suhrbler. 1982. Isolation of mutagenic amines from a coal conversion oil by cation exchange chromatography. Anal. Chem. 54:32-37.

Ho C., B. T. Walton, G. L. Kao, and M. R. Guerin. 1984. Identification of benzo(g)isoquinoline-5-10 dione as an insect teratogen in commercial acrinie, Environ Sci. Technol. 18:362.

Godsy, E. M., D. F. Goerlitz, and D. Grbic-Galic. 1993. Methanogenic degradation kinetics of nitrogen and sulfur containing heterocyclic aromatic compounds in aquifer-derived microcosms. In: Symposium on Bioremediation of Hazardous Wastes: Research Development, and Field Evaluations. EPA/600/R-93/054, pp. 123-128.

Jorgensen, A. D., J. R. Stetter, and V. C. Stamoudis. 1985. Interactions of aqueous metal ions with organic compounds found in coal gasification: model systems. Environ. Sci. Technol. 19(10):919-924.

Klaassen, C. D., M. O. Amdur, and J. Doull. 1986. Casarett and Doull's Toxicology. The Basic Science of Poisons. Macmillan Publishers, Toronto, Canada.

Krone, C. A., D. G. Burrows, D. W. Brown, P. A. Robisch, A. J. Friedman, and D. C. Malins. 1986. Nitrogen-containing aromatic compounds in sediments from a polluted harbor in Puget Sound. Environ. Sci. Technol. 20(11):1144-1150.

Laha, S. and R. G. Luthy. 1990. Oxidation of aniline and other primary aromatic amines by manganese dioxide. Environ. Sci. Technol. 24(3):363-367.

Lehr, R. E. and D. M. Jerina. 1983. Aza-polycyclic aromatic hydrocarbon carcinogenicity: predictions of reactivity of tetrahydrobenzo ring epoxide derivatives, Tetrahedron Letts. 24(1):27-30.

Leo, A., C. Hansch, and D. Elkins. 1971. Partition coefficients and their uses. Chem. Rev. 71(6):525-616.

Lopez-Avila, V. and R. A. Hites. 1980. Organic compounds in an industrial wastewater. Their transport into the sediments. Environ. Sci. Technol. 14(11):1382-1390.

Lui, D., and B. J. Dutka (eds). 1987. Toxicity screening procedures using bacterial systems. Marcel Dekker, NY, 475 pp.

Malins, D. C., M. M. Krahn, M. S. Meyers, L. D. Rhodes, D. W. Brown, C. A. Krone, B. B. McCain, and S. -L. Chan. 1985. Toxic chemicals in sediments and biota from a creosote-polluted harbor: relationships with hepatic neoplasms and other hepatic lesions in English sole, Carcinogenesis 6(10):1463-1469.

Maron, D. M. and B. N. Ames. 1983. Revised methods for the Salmonella mutagenicity test, Mutation Res. 113:173-215.

McCann, J., E. Choi, E. Yamasaki, and B. N. Ames. 1975. Detection of carcinogens as mutagens in the Salmonella/microsome test: assay of 300 chemicals. Proc. Nat. Acad. Sci. USA, 72(12):5135-5139.

McFall, J. A., S. R. Antione, and I. R. DeLeon. 1985. Base neutral extractable organic pollutants in biota and sediments from Lake Pontchartrain. Chemosphere 14(10):1561-1569.

McLafferty, F. W. 1980. Interpretation of mass spectra (3rd Edition), University Science Books, Mill Valley, CA, 303 pp.

Millar, C. E., L. M. Turk, and H. D. Foth. 1986. Fundamentals of soil science (4th Edition), John Wiley and Sons, Inc. NY.

Ortiz de Montellano, P. R. (ed). 1986. Cytochrome P-450. Structure, Mechanism, and Biochemistry. Plenum Press, NY, pp. 275-300.

Parris, G. E. 1980. Covalent binding of aromatic amines to soil humates. I. Reaction with carbonyls and quinones. Environ. Sci. Technol. 14:1099-1106.

Patrick, W. H., B. G. Williams and J. T. Moraghan. 1973. A simple system for controlling redox potential and pH in soil suspensions, Proc. Soil Sci. Soc. America, 37(2):331-2.

Philips, D. H. 1983. Fifty years of benzo(a)pyrene. Nature 13:408-412.

Ponnamperumma, F. N. 1972. The chemistry of submerged soils. Adv. Agron. 24:29-96.

Poole, C. F. and S. K. Poole. 1991. Chromatography Today, Elsevier Science Publ., NY, 1026 pp.

Roubal, W. T. and D. C. Malins. 1985. Free radical derivatives of nitrogen heterocycles in livers of English sole (Parophys vetulis) with hepatic neoplasms and other liver lesions. Aquatic Toxicol. 6:87-103.

Smith, J. H., W. R. Mabey, N. Bohonos, B. R. Holt, S. S. Lee, T. -W. Chou, D. C. Bomberger, and T. Mill (1977, 1978). Environmental pathways of selected chemicals in freshwater systems, Parts I and II, EPA 600/7-77-113 and 600/7-78-074, respectively.

Stetter, J. R., V. C. Stamoudis, and A. D. Jorgensen. 1985. Interactions of aqueous metal ions with organic compounds found in coal gasification: process condensates. Environ. Sci. Technol. 19(10):924-928.

Sumskaya, A. I. and D. F. Varfolomeyev. 1988. Identification of petroleum products contained in biologically purified refinery effluent. Petrol. Chem. USSR, 28(3):167-176.

Thompkins, B. A. and C. Ho. 1982. Determination of polycyclic aromatic amines in natural and synthetic crudes, Anal. Chem. 54:91-96.

Turov, Y. P., N. N. Gerasimova, T. A. Sagachenko, and O. A. Bieko. 1987. Group composition of the low molecular weight nitrogen bases of Samotlor crude oil. Petrol. Chem. USSR, 27(1):20-25.

Wakeham, S. G. 1979. Azaarenes in recent lake sediments. Environ. Sci. Technol. 13(9):1118-1123.

Walton, B. T. and T. Mill (1988). Structure activity relationships in environmental toxicology and chemistry, Environ Toxicol. Chem. 7:403-404.

Weber, E. J., D. L. Spidle, and K. A. Thorn. 1993. Bioremediation of soils and sediments contaminated with aromatic amines. In: Symposium on bioremediation of hazardous wastes: research development and field evaluations (Abstracts), EPA/600/R-93/054, pp. 137-138.

Werstiuk N. H. and T. Kadai (1974). The high temperature and dilute acid (HTDA) procedure as a general method of replacing aromatic hydrogen by deuterium. *Can. J. Chem.*, 52:2169-71.

Wolfe, D. A. (ed.) 1977. Fates and effects of petroleum hydrocarbons in marine organisms and ecosystems. Pergamon Press, NY, 478 pp.

Yamaguchi, T. and T. Handa. 1987. Characterization of aza heterocyclic hydrocarbons in particulate matter, Environ. Sci. Technol. 21(12):1177-81.

Zitko, V. 1980. The analysis of aquatic sediments for organic compounds. In: Baker, R. A. (ed.), Contaminants and sediments, volume 2: analysis, chemistry and biology. Ann Arbor Science Publishers, Ann Arbor, MI, pp. 89-99.

The Department of the Interior Mission

As the Nation's principal conservation agency, the Department of the Interior has responsibility for most of our nationally owned public lands and natural resources. This includes fostering sound use of our land and water resources; protecting our fish, wildlife, and biological diversity; preserving the environmental and cultural values of our national parks and historical places; and providing for the enjoyment of life through outdoor recreation. The Department assesses our energy and mineral resources and works to ensure that their development is in the best interests of all our people by encouraging stewardship and citizen participation in their care. The Department also has a major responsibility for American Indian reservation communities and for people who live in island territories under U.S. administration.

The Minerals Management Service Mission

As a bureau of the Department of the Interior, the Minerals Management Service's (MMS) primary responsibilities are to manage the mineral resources located on the Nation's Outer Continental Shelf (OCS), collect revenue from the Federal OCS and onshore Federal and Indian lands, and distribute those revenues.

Moreover, in working to meet its responsibilities, the **Offshore Minerals Management Program** administers the OCS competitive leasing program and oversees the safe and environmentally sound exploration and production of our Nation's offshore natural gas, oil and other mineral resources. The MMS **Royalty Management Program** meets its responsibilities by ensuring the efficient, timely and accurate collection and disbursement of revenue from mineral leasing and production due to Indian tribes and allottees, States and the U.S. Treasury.

The MMS strives to fulfill its responsibilities through the general guiding principles of: (1) being responsive to the public's concerns and interests by maintaining a dialogue with all potentially affected parties and (2) carrying out its programs with an emphasis on working to enhance the quality of life for all Americans by lending MMS assistance and expertise to economic development and environmental protection.